Bulletin of the Seismological Society of America

A Scientific Vision and Roadmap for Earthquake Rupture Forecast Developments, a USGS Perspective

--Manuscript Draft--

Manuscript Number:	BSSA-D-24-00217R2
Article Type:	Article
Section/Category:	Regular Issue
Full Title:	A Scientific Vision and Roadmap for Earthquake Rupture Forecast Developments, a USGS Perspective
Corresponding Author:	Edward H. Field, Ph.D. USGS Pasadena, CA UNITED STATES
Corresponding Author's Institution:	USGS
Corresponding Author E-Mail:	field@usgs.gov
Order of Authors:	Edward H. Field, Ph.D.
	Alexandra Hatem
	Bruce Shaw
	Morgan Page
	P. Martin Mai
	Kevin Milner
	Andrea Llenos
	Andrew Michael
	Fred Pollitz
	Jessica Thompson Jobe
	Tom Parsons
	Olaf Zielke
	David Shelly
	Alice-Agnes Gabriel
	Devin McPhillips
	Richard Briggs
	Elizabeth Cochran
	Nicolas Luco
	Mark Petersen
	Peter Powers
	Justin Rubinstein
	Allison Shumway
	Nicholas van der Elst
	Yuehua Zeng
	Christopher Duross
	Jason Altekruse
Abstract:	We articulate a scientific vision and roadmap for the development of improved

	Earthquake Rupture Forecast (ERF) models, which are one of the two main modeling components used in modern seismic hazard and risk analysis. One primary future objective is to provide fully time-dependent models that include both elastic rebound and spatiotemporal clustering nationwide, which can be particularly important for shorter-term hazard and risk considerations (e.g., earthquake insurance products). We also discuss the importance and perennial challenges associated with quantifying epistemic uncertainties, including those associated with deformation-model slip rates, un-quantified sampling errors with respect to off-fault seismicity, and any spatial covariances. The need for more physics-based approaches is also emphasized, as is the benefit of adding model valuation (quantifying usefulness) to our verification and validation protocols. Given the multidisciplinary and system-level nature of this activity, modular design is critical. Future updates will also draw from best-available science by both the U.S. Geological Survey and the external community. The primary goal of this paper is to highlight plans that guide research and facilitate community engagement with model development, especially with respect to lowering the entry barrier for early career scientists and engineers. The paper is written so readers can focus on the sections that interest them most (see table of contents), with the Introduction and Discussion providing a stand-alone overview and summary.
Author Comments:	Sorry for the delay, but the DOI approval process for this one was brutal. It has been edited accordingly, and some figures have also been updated, but nothing substantial has changed. I could only submit a jpg version of Figure 2 because the PDF and AI files exceed the size limit. I can modify the latter if I get instructions on how to do so (or I give a link to the PDF below). I was going to suggest Figure 2 as a cover image, but I see the latter cannot be a figure from the paper. Please handle the TOC something like you did in https://doi.org/10.1785/0120230120. Thanks for your patience! An editable copy of Figure 2 is available here: https://1drv.ms/b/c/80b7c558b10c7262/ESoduQg1tjFHliazoZ0RYewBPmcMKTXe6dMFzCQx61Vkng?e=zzWMUw
Suggested Reviewers:	
Opposed Reviewers:	
Response to Reviewers:	
Additional Information:	
Question	**Response**
Key Point #1: <i>Three key points will be printed at the front of your manuscript so readers can get a quick overview. Please provide three COMPLETE sentences addressing the following: 1) state the problem you are addressing in a FULL sentence; 2) state your main conclusion(s) in a FULL sentence; and 3) state the broader implications of your findings in a FULL sentence. Each point must be 110 characters or less (including spaces).	A roadmap for ERF developments; these are one of the two main modeling components used in SHA
Key Point #2:	A main goal is developing fully time-dependent models (both elastic rebound and spatiotemporal clustering)
Key Point #3:	Another main goal is more complete epistemic uncertainty representation

A Scientific Vision and Roadmap for Earthquake Rupture Forecast Developments, a USGS Perspective

Edward H. Field, Alexandra E. Hatem, Bruce E. Shaw, Morgan T. Page, Martin Mai, Kevin R. Milner, Andrea L. Llenos, Andrew J. Michael, Fred F. Pollitz, Jessica Thompson Jobe, Tom Parsons, Olaf Zielke, David R. Shelly, Alice-Agnes Gabriel, Devin McPhillips, Richard W. Briggs, Elizabeth S. Cochran, Nicolas Luco, Mark D. Petersen, Peter M Powers, Justin L. Rubinstein, Allison M Shumway, Nicholas J. van der Elst, Yuehua Zeng, Christopher B. Duross, and Jason M. Altekruse

Corresponding Author: Edward (Ned) Field (field@usgs.gov)

Abstract

We articulate a scientific vision and roadmap for the development of improved Earthquake Rupture Forecast (ERF) models, which are one of the two main modeling components used in modern seismic hazard and risk analysis. One primary future objective is to provide fully time-dependent models that include both elastic rebound and spatiotemporal clustering nationwide, which can be particularly important for shorter-term hazard and risk considerations (e.g., earthquake insurance products). We also discuss the importance and perennial challenges associated with quantifying epistemic uncertainties, including those associated with deformation-model slip rates, un-quantified sampling errors with respect to off-fault seismicity, and any spatial covariances. The need for more physics-based approaches is also emphasized, as is the benefit of adding model valuation (quantifying usefulness) to our verification and validation protocols. Given the multidisciplinary and system-level nature of this activity, modular design is critical. Future updates will also draw from best-available science by both the U.S. Geological Survey and the external community. The primary goal of this paper is to highlight plans that guide research and facilitate community engagement with model development, especially with respect to lowering the entry barrier for early career scientists and engineers. The paper is written so readers can focus on the sections that interest them most (see table of contents), with the Introduction and Discussion providing a stand-alone overview and summary.

Table of Contents

109
110

Introduction & Background

The Congressionally enacted Earthquake Hazards Reduction Act of 1977 and subsequent reauthorizations give the U. S. Geological Survey (USGS) statutory responsibility to study, monitor, broadcast, and forecast earthquake activity, which it accomplishes via the USGS Earthquake Hazards Program (Hayes et al., 2024). With respect to forecasting, the USGS produces official seismic hazard assessments, which quantify the probability of future ground shaking levels throughout the country (see **Figure 1** for USGS regions of purview). These results are used in various earthquake risk mitigation efforts, including building code design requirements and various types of earthquake insurance products. The USGS also participates in various earthquake risk analyses, which help quantify threats and consequences associated with the built environment (e.g., Jaiswal et al., 2023).

Seismic Hazard Model Components

As depicted in **Figure 2**, modern seismic hazard assessment relies on two main modeling components: 1) an Earthquake Rupture Forecast (ERF), which defines the probability of every possible fault-rupture event in a region and over a specified timespan (or a suite of synthetic catalogs of such events); and 2) a Ground Motion Model (GMM), which provides a probability distribution of possible shaking at one or more sites for a given fault rupture (or a suite of synthetic seismograms, which can be used to infer a probability distribution). While the division between ERFs and GMMs is somewhat artificial (i.e., these components could eventually be merged) the distinction will likely remain both crucial and useful for at least another decade. This report is focused on ERF development, although the themes addressed in this Introduction apply equally well to GMMs.

A few decades ago, both ERF and GMM models were relatively simple (e.g., a single individual or group could construct both), but today, as we add more realism, these models are much more "system level" in terms of requiring integration and consistency among a broad range of disciplines (e.g., seismology, geology, geodesy, and earthquake physics, as illustrated at the top of **Figure 2**). Furthermore, while in the past these models primarily influenced a single flagship product (the National Seismic Hazard Model (NSHM); e.g., Petersen et al., 2023), they are now applicable to an increasing wide array of applications, such as operational earthquake forecasting (real-time information on evolving event sequences; Jordan and Jones, 2010; Jordan et al., 2014), as a Bayesian prior for earthquake early warning (e.g., Cua and Heaton, 2007), and for hazard assessments related to tsunamis, landslides, and liquefaction.

Biggest Potential Improvements to Seismic Hazard Models

All models embody assumptions, approximations, and data uncertainties, so we are perpetually on the lookout for potential enhancements. Currently, both ERFs and GMMs have a single, major improvement that could be made. For ERFs, this is adding full time-dependence. Thus far, our NSHMs have generally been based on time-independent ERFs, especially in terms of ignoring the spatiotemporal clustering of earthquakes (e.g., aftershocks, which can be large and damaging). While these approximations are certainly more adequate for the 50-year durations and low exceedance probabilities considered in typical building codes (the traditional use of NSHMs; e.g., Building Seismic Safety Council, 2020; Luco et al., 2015), time-dependent effects may be consequential for the shorter-term hazard or risk estimates relevant to, for example, earthquake insurance and catastrophe bonds (e.g., Goda et al., 2014), response and recovery efforts (e.g., Gerstenberger et al., 2014; Bazzurro et al., 2006), and building codes for temporary structures (e.g., Mohammadi, 2008). Time-dependence may also be impactful for the higher 50-year exceedance

probabilities in building codes governing the retrofit of existing structures (e.g., American Society of Civil Engineers, 2023), the design of tall buildings (e.g., Pacific Earthquake Engineering Research Center, 2017), and community resilience (e.g., NIST-FEMA, 2021; Blowes et al., 2023).

Figure 3 illustrates how spatiotemporal seismicity clustering influences earthquake rates (and the probability of large events by proxy) over a 100-year period, revealing not only order-of-magnitude rate increases following large events, but relatively quiet times as well (see caption for details). The general rule of thumb is that every earthquake has about a 5-10% chance of being followed by something even larger in the week that follows (Reasenberg and Jones, 1989, 1994), which has been borne out by numerous large-event sequences. This means the 1-year likelihood of fatalities and financial losses can increase by an order of magnitude following a large mainshock, whereas earthquake loss modelers typically find 10% changes actionable (e.g., Field, Porter, et al., 2017). Our current official hazard models ignore this time dependence, which is why the 2023 USGS NSHM explicitly states that applicability is restricted to return periods above ~475 years (Petersen et al., 2023). Addressing this limitation is a major theme of this paper.

With respect to GMMs, the most impactful improvement will be to relax the so-called "ergodic" assumption (Anderson and Brune, 1999), which basically means developing rupture- and site-specific GMMs (or path-specific models if "path" implicitly includes source and site effects). The seismic-hazard calculation for a site involves considering the ground motion produced by every possible earthquake rupture (defined by the ERF). Therefore, we would ideally have multiple realizations of the ground motion produced at each site and for each rupture. Unfortunately (from a predictability perspective), only a tiny fraction of ERF-represented ruptures has actually occurred, and those that have produced observed data at only a tiny fraction of sites. Thus, empirical GMMs have been forced to aggregate the limited data by magnitude, distance, and a few other variables, and to apply the consequent, collective variability to that assumed for each unique rupture and site

combination. Were we ever to obtain enough recordings, however, we would surely discover that ground motions for each specific rupture and site combination are systematically higher or lower, and less variable, than implied by this "ergodic" model. Efforts to relax this assumption have demonstrated that doing so can have a dramatic influence on inferred hazard (e.g., Wang and Jordan, 2014; Abrahamson et al., 2019).

Uncertainty Quantification

The hazard and risk posed by an earthquake generally increases with magnitude, which poses a perennial challenge in that the paucity of larger magnitude events means we are constructing and testing models with sparse datasets. One consequence and challenge is a need to quantify forecasting uncertainties, especially given inevitable modeling assumptions, approximations, and input data limitations. Such uncertainties are referred to as "epistemic" (due to a lack of knowledge, which means they could be reduced with further study) in contrast to "aleatory" uncertainty (intrinsic variability built into a model representing luck of the draw, which cannot be reduced with more information). This distinction is model dependent in that aleatory uncertainty can, for example, get converted to epistemic as more parameters are added to a model (see Marzocchi and Jordan (2018) for an advanced discussion).

The bottom line is an ERF, or any model for that matter, is limited and questionable without some indication of epistemic uncertainties. These are traditionally represented with a logic tree, in which branches represent the set of options and relative weights (the likelihood of being correct) for each uncertain model element (see Figure 5 of Petersen et al. (2023) for an example). The result is some generally large number of alternative models representing the range of possibilities. Ideally this set is mutually exclusive and collectively exhaustive, but this is usually difficult to achieve due to, for example, unanticipated correlation among branches and unknown unknowns

(missing branches). Full-disclosure obligations dictate that we nevertheless do the best we can, and while we continually make significant progress, defining an adequately complete and computationally manageable set of branches remains a grand and perennial challenge. A practical manifestation is that our forecasting uncertainties are generally still growing with each new model, whereas we want to get to where new research reduces overall uncertainties. A related challenge is that regions with less information may imply less uncertainty, whereas the opposite should be true.

Physics-Based Modeling

Another consequence and challenge due to limited large-magnitude data is a need for more physics-based modeling approaches, which effectively enable inferences where we lack adequate observations to constrain statistical models. However, physics-based modeling presents its own set of challenges including: having an adequate understanding and numerical representation of the physical process; developing and maintaining advanced computational platforms; access to rapidly evolving high-performance-computing facilities; management and processing of massive data sets; representing and propagating epistemic uncertainties; and maintaining reproducibility. For these reasons, the USGS relies heavily on external collaborations to develop and maintain such capabilities. Ultimately, physics-based models could be used directly for hazard and risk estimation, but this is probably at least a decade away. For now, we use them to help guide the functional form of more empirical, traditional models. Nevertheless, it is hard to imagine an activity that will have a greater impact on what earthquake hazard models look like 20 years from now given the rarity of large, damaging events.

Basic Research

A key to success with respect to the above model-development challenges is having a strong and robust earthquake research program, both with respect to identifying and testing the various scientific hypotheses underpinning the range of viable models, but also with respect to developing more physics-based approaches. This obviously includes focus on model elements deemed "best-available science" (defined in Jordan et al. (2023)) with respect to current applications, but also more exploratory or curiosity-driven science to enable unanticipated innovations. It is also important to recognize that system-level ERF and GMM models serve not only practical applications, but also form a crucial basis for investigating and testing scientific hypotheses. More specifically, the process of combining insights from different disciplines (system-level model construction) often reveals incompatibilities that trigger new investigations that help resolve outstanding questions much more efficiently than siloed disciplines ever could.

Verification, Validation, and Valuation

Another key to ERF development is having robust verification, validation, and valuation protocols. Verification ensures our models are implemented as intended (e.g., code debugging). Validation is the extent to which the models are consistent with nature, which is challenging given a paucity of data at the large magnitudes that dominate hazard, as discussed more below.

Valuation is a relatively new concept (e.g., Jordan et al., 2011) born out of the phrase "all models are wrong ... some are useful" (Box, 1980). More specifically, given all models embody assumptions, approximations, and data uncertainties, perhaps the most relevant question is whether a new or competing model represents value added (e.g., does the increased usefulness outweigh the cost of development and maintenance?). The answer to this question depends on the particular use (e.g., building codes, earthquake insurance, catastrophe bonds). As already noted, our NSHMs have effectively been tailored for building codes (time-independent, individual site hazard curves). More

specifically, questions arose following the release of the 2023 NSHM (Petersen et al., 2023) on whether the model is appropriate for shorter-term and/or spatially distributed hazard and risk metrics, which represents a significant issue for the insurance community (e.g., Jordan et al, 2023). Broader valuation depends on having an operationalized ability to compute an adequate range of hazard and risk metrics during model development, which is currently a work in progress. Such valuations can also identify which uncertain model elements are most impactful with respect to real-world decisions, which feeds back to identifying which scientific studies might be most beneficial. This would also sharpen any research priority statements that are currently based on informed speculation.

Objectives Of This Document

The purpose of this ERF-development roadmap is to: 1) articulate goals, priorities, and opportunities (low hanging fruit); 2) identify and track the various modular elements that need to be developed and integrated; 3) clarify how potential participants may contribute; and 4) identify model aspects that need particular attention. This effort builds on accomplishments and lessons learned from the time-independent ERFs developed for the USGS NSHM (Petersen et al., 2023), including and ERF model for Hawaii (Petersen et al., 2021), Alaska (Powers et al., 2024), and the Conterminous United States (Field et al., 2023, referred to hereafter as 2023-CONUS-ERF-TI, in which "TI" indicates time independence). The latter also provides a comprehensive overview of these efforts, including model component and construction details, the contributions represented by more than 25 supporting publications, and an unprecedented review process (Jordan et al. (2023), which was particularly influential on the views represented here). We admit this is a USGS-centric roadmap and acknowledge that other countries have some unique issues and perspectives

(e.g., Gerstenberger et al., 2020; Meletti et al., 2021; Gerstenberger et al., 2023; Danciu et al., 2024; Mizrahi et al., 2024), which are not addressed or debated here. We also emphasize that this paper does not represent a comprehensive review of related research; rather, we cite papers that provide more information on each topic at hand.

Mindful that many readers will not want to read this entire document, it has been written so that the Introduction and Discussion sections stand alone with respect to key, general points (leading to some redundancy for those reading the entire document). There is also an uneven level of detail among sections, as our primary focus here is on ERF construction. For example, we often describe what is needed from the various disciplinary groups (e.g., improved slip-rate uncertainties from tectonic geodesy) without detailed guidance on how to achieve these goals. Likewise, we do not elaborate on exactly how to improve model testing, the review process, formalized expert solicitation (SSHAC, Cooke, Delphi, etc.), product dissemination and public messaging, or exactly what types of risk metrics that may deserve more scrutiny during model development. Again, this is partly to avoid discussing reasonable debates surrounding these topics, all of which are more general in terms of being applicable to GMMs as well. Likewise, we do not discuss site-specific hazard analysis (in which practitioners go above and beyond the NSHM model with more detailed, local information), other than to note that the USGS is open to incorporating what is learned into our future NSHMs.

Several of our previously stated general goals were largely accomplished (Field et al., 2023), including a de-regionalization of model-component development (to eliminate spatial variability due merely to differing opinions), broader involvement of external collaborators and personnel across the Earthquake Hazards Program (beyond the NSHM project), and extensibility with respect to adding time dependence.

Broader goals that were partially fulfilled but are still a work in progress include:

- More complete representation of epistemic uncertainties
- Removal of previously applied complexities that no longer provide added value
- Maximizing uniformity of model components and simultaneous updates across regions
- More operationalization of model-component development (i.e., push-button updates)
- Improved documentation with respect to implementation and reproducibility
- Enabling customized solutions for users (e.g., a consultant that wants to change a slip rate constraint in a fault-system solution)
- Better robustness with respect to personnel departures

All these goals are discussed more extensively by Field et al. (2023) and exemplified below.

ERF Construction (Main Model Elements)

Given the system-level nature of ERF development, a modularized construction is critical to keep things manageable and to enable different groups of scientists to focus within their respective areas of expertise. The top-level model components utilized here, and depicted in **Figure 4**, include Fault Model(s), Deformation Model(s), Earthquake Rate Model(s), and Earthquake Probability Model(s). **Figure 4** also illustrates that multi-cycle physics-based simulators could be substituted for the earthquake rate and probability components. Fault Models provide the three-dimensional (3D) spatial representation of explicitly modeled faults. Deformation Models supply at least slip-rate estimates on these fault planes, but ideally the deformation occurring off these faults in surrounding regions as well. The Earthquake Rate Model gives the long-term rate of every modeled earthquake rupture in the region (at some finite discretization level), which is sufficient for a time-

independent ERF. The Earthquake Probability Model states the likelihood of each rupture conditioned on other information, such as time since last event on faults and/or the behavior of nearby seismicity. In sum, the consequent ERF essentially provides the probability of every modeled rupture for a specified timespan (a list of all potentially consequential events) or sets of synthetic catalogs for the timespan (also referred to as "stochastic event sets" in risk modeling). Multi-cycle physics-based simulators generate synthetic catalogs by modeling the stress accumulation on faults, the frictional properties leading to rupture, and the stress transfer caused by each earthquake.

Each of these elements is discussed in a dedicated section below, followed by further discussions of operational earthquake forecasting (OEF), model testing and valuation, the computational infrastructure, and the review process. Note that we do not categorize discussions by tectonic region type (active crustal, stable continental, subduction zone, etc.), but rather mention any associated, unique challenges where appropriate.

Fault Models

A fault model comprises the 3D geometry of explicitly modeled faults (see Hatem et al. (2022) and Thompson Jobe et al. (2022) for recent examples). More specifically, a fault model is a list of fault sections that collectively represent a viable depiction of the known fault system (alternative interpretations, meaning epistemic uncertainties, are represented with separate fault models). In its simplest form, a fault section is composed of:

- Fault trace (defined by a list of geographic locations)
- Average fault dip and dip direction

- Average upper and lower seismogenic depths
- A geologically inferred average rake

Fault sections vary widely in length, and some can be quite long (over 200 km) if associated attributes do not vary along strike. More complicated, non-planar fault surfaces (e.g., subduction zones or listric faults) can be represented with triangular surfaces, or by defining an upper and lower fault trace (reflecting upper and lower seismogenic depths) together with the depths for a set of points on the fault surface (e.g., evenly discretized when projected to the Earth surface).

What's really down there?

The adage that all models represent an approximation of the real system is especially true for faults. A fundamental challenge is our limited understanding of what faults look like at depth, including the dip and its potential variation along strike. Is a given fault a single, well-defined surface, or a labyrinth of interconnected micro surfaces, and what about connectivity between neighboring faults? How much does this vary throughout the system, or even along a single fault? Efforts to constrain fault surfaces at depth include examinations of seismicity, seismic reflection data, and borehole studies, all of which provide only a limited view. With respect to distinguishing areas where faulting is highly distributed, as opposed to a well-defined trace, a fault-zone polygon is typically defined (and sometimes centered on a proxy fault). The question of where one fault ends and another begins is critical with respect to the likelihood of multi-fault ruptures, raising the issue of exactly how to best represent such uncertainties.

What level of detail?

Information on surface fault traces can be relatively detailed, especially when documented immediately following a (large) earthquake that ruptured to Earth's surface. In addition to whether this detail projects to depth, as already noted, there is also the question of how repeatable it is between earthquakes (versus more chaotic behavior due to shallow geologic heterogeneities and free surface effects). Sensitivity tests show that hazard maps are generally insensitive to these details, mostly because ground-motion models effectively smooth results over several kilometers. However, greater detail will presumably be influential and appropriate for fault displacement hazard and when utilizing more physics-based models.

How many faults to include?

Given most earthquakes are caused by fault rupture, and we acknowledge that such earthquakes can occur almost anywhere (modeled with off-fault gridded seismicity discussed below), there are certainly many more faults than possibly can be identified. Also, some of those we know about may be dormant or insignificant with respect to hazard. On the other hand, adding a fault to a fault model may be consequential in terms of increasing inferred hazard. Decisions on which faults to include are often based on subjective judgements, time constraints, and/or resource limitations. Valuation analyses and sensitivity tests would help make such decisions more quantitative, although we would need to ensure that such interpretations are applicable for all hazard and risk metrics of potential interest.

Upper and lower seismogenic depths?

Upper and lower seismogenic depth is another consequential, yet poorly understood concept. It is meant to define the bounds of dynamic rupture, meaning any fault offset occurring above and

below this range represents stable slip that does not generate damaging seismic waves. One problem is this boundary is probably not abrupt, but rather a zone of transition between stable and unstable slip. Another is the possibility that this zone varies between earthquakes (e.g., larger earthquakes may reach below the lower seismogenic depth due to conditional stability of dynamic rupture). These questions are intertwined with how creep is handled in deformation models and how scaling relationships convert rupture area to magnitude, both of which are discussed below.

Alternative Fault Models?

All the above uncertainties can be represented by defining alternative Fault Models and assigning a relative probability that each is correct (logic-tree branches representing epistemic uncertainties). That said, the number of alternative Fault Models was actually reduced to zero in the latest NSHM, mostly because the impact of available options was generally minimal with respect to several hazard and risk metrics (Field et al., 2023). This reversal does not mean these uncertainties are negligible, but rather reflects the triage mode with respect to addressing the most consequential issues. In addition, one should not presume that the insensitivities inferred for limited set of hazard and risk metrics examined thus far will apply to all other metrics. Furthermore, many of these questions will be much more relevant for physics-based models, including the sensitivity of multi-fault ruptures to geometric and jump-distance details between faults. Alternatively, physics-based models may be our best option for addressing some of the questions raised here, such as how dynamic rupture transitions to stable slip near upper and lower seismogenic depths.

In summary, it is essential to remain vigilant with respect to fault model uncertainties (e.g., by conducting sensitivity tests with alternative representations), but also to acknowledge that there will always be upper limits on what we will ever know (and plan ERF development accordingly).

Deformation Models

Deformation Models provide, for a given Fault Model, slip-rate, rake, and creep-rate estimates for each fault section, plus the spatial distribution of "off-fault" deformation (if produced by the model). Those utilized in the western U.S. portion of the 2023-CONUS-ERF-TI are described in a special issue of *Seismological Research Letters* (see Pollitz et al. (2022) for the overview paper). The inputs to these models, in addition to a Fault Model, are typically the following:

1) Geologic slip-rate estimates, including uncertainties, at points on faults (e.g., Hatem et al., 2022), which are either explicit constraints if site-specific geologic studies are available, or categorical proxy estimates if studies are lacking (based on analogous faults).
2) Global Navigation Satellite System (GNSS) velocity vectors (e.g., Zeng, 2022a).
3) "Ghost transient" corrections for time-dependent effects caused by viscoelastic relaxation following large historic events (Hearn, 2022)
4) Fault creep inferences (e.g., Johnson et al., 2022).

The five different deformation models developed for the 2023-CONUS-ERF-TI highlight several issues that can benefit from further study. First, there was often a very high and consequential

degree of variability among models in terms of best-estimate slip rates, governed largely by how much each model was forced to match the geologic slip-rate constraint. Models that weighted mean geologic values heavily were largely in agreement, whereas those that were less stringent (e.g., with a more uniform prior with respect to geologic uncertainties) were more variable. Results from the latter were often referred to as "outliers" but this does not necessarily mean they are wrong (as reflected by the fact that such models were given low but non-zero weight).

Improved Epistemic Uncertainty Representation in Deformation Modeling

The fundamental question is how any underdetermined slip rates are being handled, particularly if geologic uncertainties are large and GNSS constraints are sparse. In this case, there will be a range of slip rates that fit the data equally well (the so-called null space from inverse theory). To borrow an example from Field et al. (2023), consider two closely spaced parallel faults with no geologic slip-rate constraints (or very large uncertainties), but nestled between two GNSS stations. These faults would exhibit a near-perfect slip-rate tradeoff in terms of satisfying the GNSS deformation (e.g., a maximum slip rate on one with a minimum on the other, or vice versa, or any linear combination of these two models, would fit the data equally well). To reflect such tradeoffs, multiple realizations from each deformation model would be required to map out the complete range of viable models (effectively representing the slip-rate covariance between faults). Instead, we presently have a "best estimate" from each of the five western U.S. models, and it is highly doubtful that this set represents the complete range of possibilities.

Improved Ghost Transient Corrections

460

461 The deformation models for the 2023 NSHM effort accounted for ghost transients contributed by
462 earthquake cycles on separate source areas for the southern San Andreas Fault (SAF), the northern
463 SAF, and the Cascadia megathrust (Hearn, 2022). This correction accounts for time-dependent
464 deformation during any individual cycle and quantifies the transient at a given time (e.g., the GNSS
465 observation periods used for the input data) referenced to the expected secular deformation
466 contributed by that cycle. While the employed corrections in the 2023 NSHM effort covered major
467 fault cycles and improved the deformation models' fit to the data, questions arise as to the accuracy
468 of the correction and whether cycles from additional faults, e.g., along the northern Eastern
469 California Shear Zone (cycles of 1872 Owens Valley-type earthquakes), could be further significant
470 contributions. Resolving these questions could require examination of more sophisticated
471 viscoelastic deformation structures, numerical models that employ these structures, and assembly
472 of relevant parameters describing additional earthquake cycles (e.g., Guns et al., 2021; Young et al.,
473 2023).

474 **Usefulness of off-fault deformation?**
475

476 Four of the western U.S. deformation models also provided estimates of off-fault deformation
477 (meaning distributed diffuse deformation that is not accounted for by explicitly modeled faults).
478 Figure 14 of Pollitz et al. (2022) or Figure 4 of Johnson et al. (2023) reveal a high degree of off-fault
479 variability between models. Unfortunately, and as in the previous Uniform California Earthquake
480 Rupture Forecast, Version 3 effort (UCERF3; Field et al., 2014), it is not clear how much of the
481 implied features are real versus artifacts of model assumptions and approximations; hence, this
482 information could not be used to estimate the rate of off-fault seismicity (as an alternative to the
483 traditional smoothed-seismicity approach discussed below). This is consistent with

recommendations of the deformation model review team (Johnson et al., 2023), who also discuss what it might take to improve such estimates.

The previous UCERF3 effort also had the intriguing implication that 30% to 60% of the off-fault moment rate predicted by deformation models must be aseismic (the maximum magnitudes required to satisfy full moment rates were unrealistically high). Not only was this issue never resolved, but it has not yet been fully examined for the new deformation models. Another question is the extent to which block rotations can soak up shear strain without contributing to fault slip rates.

Earthquake Rate Models

An earthquake rate model gives the long-term rate of every modeled earthquake rupture in a region and at some level of space-time discretization. The model is essentially a list of "sources," where each source represents a collection (or list) of related ruptures. The two main types of sources are off-fault gridded seismicity and fault-based sources, where the latter is further divided into classic fault sources, fault-zone sources, and fault-system solutions (the last one to represent multi-fault ruptures). Field et al. (2023) give an in-depth description of each source type, as well as implementation details for those utilized in the 2023-CONUS-ERF-TI. We do not repeat descriptions of classic fault sources here because they are simple and also represented in the fault-system-solution framework. Advantages of the latter include automatic computing of various diagnostics (e.g., implied slip rates), accommodating time dependence when desired, and applicability to fault systems in any type of tectonic region. Fault-zone sources are also conceptually simple, thus, we do not discuss their implementation details either.

A fault-system solution, which represents the rate of large earthquakes throughout an interconnected fault system, is specified by:

1) a list of fault subsections (same finite-surface representation as described in Fault Models section above)
2) a list of fault ruptures (each of which has a magnitude, long-term rate, average rake, and a finite rupture surface defined as a list of utilized subsections).

The rates of ruptures can be: 1) prescribed by imposing a specific magnitude-frequency distribution (MFD) for simple fault systems; 2) based on an inversion that is constrained to match a variety of data constraints; or 3) inferred from multi-cycle physics-based simulator results (e.g., Shaw et al., 2018; Milner et al., 2021).

Inversion-Based Fault System Solutions

Inversion-based solutions are the most general, flexible, reproducible, and comprehensive with respect to representing a full range of viable models (epistemic uncertainties). The model usually applies to "supra-seismogenic" ruptures (i.e., length ≥ full down-dip width) and event rates are inferred by satisfying various data constraints using inverse theory (**Figure 5)**. The literature on this approach is now extensive (Andrews and Schwerer, 2000; Field and Page, 2011; Field et al., 2014; Page et al., 2014; Valentini et al., 2020; Field et al., 2020a, Field et al., 2023, and Milner and Field, 2023) and we believe this type of model has received much more scrutiny than classic fault

sources. Furthermore, with recent enhancements such as full adjustability with respect to segmentation and multifault ruptures (Milner and Field, 2023), future work might amount to fine tuning and (hopefully) trimming some of the present epistemic uncertainties. Field et al. (2023) provide a comprehensive overview and Milner and Field (2023) state important implementation details, which are not repeated here. Instead, we focus on the main ingredients and possible refinements.

Defining the Rupture Set (Plausibility Filter)

Starting from a deformation model (and the associated fault model), a crucial step is defining the set of viable ruptures using a "plausibility filter" because otherwise the set can become unmanageable for large fault systems. The latest approach, developed by Milner et al. (2022), utilizes Coulomb favorability metrics, and so far, no major issues have been identified. That said, we do find specific cases that some question, usually a blockage to throughgoing rupture that geologists would like to relax (e.g. due to a fault gap being too large or Coulomb incompatibility with respect to styles of faulting). Exceptions can be made, of course, but we also want to keep things reproducible by avoiding *ad hoc* or "hard coded" exceptions. Further enhancements can be made to the plausibility filter, such as imposing a maximum rupture length (e.g., Rodriguez Padilla et al., 2024), but it is also important to keep in mind that no set of rules will be perfect, especially given inherent fault-model uncertainties.

Treatment of Fault Creep

Creep estimates, where available (e.g., Johnson et al., 2022), are used to define a *creep fraction* for each fault within each deformation model (specified relative to the slip rate). *Creep fraction* is then used to set the *aseismicity factor* and *coupling coefficient*, which are applied as a fractional reduction of seismogenic area and slip rate, respectively. For the 2023 NSHM, the first 40% of fractional creep defines a rupture-area reduction and the remainder a slip-rate reduction as follows:

$$if\ creep\ fraction \leq 0.4:$$

$$aseismicity\ factor = creep\ fraction$$

$$coupling\ coefficient = 1.0$$

$$if\ creep\ fraction > 0.4:$$

$$aseismicity\ factor = 0.4$$

$$coupling\ coefficient = 1.0 - \frac{1}{1 - 0.4}(creep\ fraction - 0.4)$$

Area reductions are accomplished by lowering the upper seismogenic depth (surface creep), and a default *creep fraction* of 0.1 is typically applied where data are lacking. Here again, no major problems have been identified, but this may be more about our limited understanding of creep and its rupture manifestations than having an unquestionable model. We also need to make sure GMMs are making consistent assumptions (e.g., with respect to depth to top of rupture).

Scaling Relationships

The magnitude of each rupture is determined from rupture area using an empirical scaling relationship, with the latest options applied in the U.S. being specified by Shaw (2023) and summarized in Field et al. (2023). Three of the models utilize a functional form of M=log(A)+c, where M and A are magnitude and area (km^2) and c is constant with values of 4.1, 4.2, or 4.3 (equally weighted) for plate boundary and intraslab events. A "Width Limited" model is also applied, for which magnitudes scale with rupture length at lower magnitudes and with down-dip width at higher magnitudes (Shaw, 2023).

Scaling relations are also used to define the average slip for each rupture (used for satisfying slip rates in the inversion), with three options being defined for NSHM 2023: 1) that implied from moment ($D_{ave} = (10^{1.5M+9.05})/(\mu A)$, where μ is shear modulus); 2) square-root length scaling ($D_{ave} = 0.22\sqrt{L}$, where L is length (km)); and 3) constant stress drop scaling (e.g., Shaw, 2023). Differences between these models reflect assumptions regarding the depth of rupture for larger events; the first option (1) assumes ruptures do not penetrate below the depth of microseismicity, producing a larger average slip than typically observed at the surface, whereas the other two options assume surface slip is consistent with that at depth and that large ruptures must therefore penetrate below microseismity depths (e.g., King and Wesnousky, 2007; Zielke et al., 2020).

We believe this set of models adequately covers the range of possibilities, so further work will hopefully trim some options, perhaps based on physics-based modeling. One exception is a possible slip-rate dependence (Anderson et al., 2021). Another is with respect to large, multifault ruptures, for which scaling might be different (observations are sparse). There also remains an alternative hypothesis that slip at a point on a fault is independent of rupture magnitude (Hecker et al., 2013), so further study may be in order.

595

596 ***Average Slip Along Rupture***

597

598 In satisfying fault slip rates from the chosen deformation model, assumptions need to be made
599 about how average slip is distributed along the rupture length. We have traditionally applied one of
600 two options: a tapered rainbow ($\sin^{1/2}$; Weldon et al., 2007) model versus a uniform (boxcar)
601 model. Only the latter option was applied in the 2023 NSHM because implied differences were
602 generally negligible, and applying the tapered model demands careful consideration of how slip
603 rates transition along strike as well. However, the biggest question is whether either of these
604 models applies to large, multifault ruptures, which might exhibit tapers at jumping points (multiple
605 rainbows). Physics-based simulators could also be useful in addressing this question.

606 ***Paleoseismic Event-Rates***

607

608 Another important set of inversion constraints are paleoseismically inferred event rates, the
609 derivation of which requires careful geologic interpretations and advanced statistical analyses (see
610 McPhillips (2022) for a recent example). If these constraints are at odds with slip rates, their
611 influence can be adjusted to provide a range of models (epistemic uncertainties). An important
612 element of this constraint is defining the probability of missed events (the fraction of ERF ruptures
613 that might have gone undetected at the paleoseismic site). We have thus far applied a simple model,
614 with a key parameter calibrated from a single San Andreas fault paleoseismic site. However, the
615 probability of missed events likely varies from site to site, according to the local depositional
616 environment and character of faulting. Another, antithetic type of uncertainty stems from the
617 potential over-interpretation of the number of inferred events at a paleoseismic site, which would
618 also be site dependent (McPhillips, 2022). Better quantification of these uncertainties could

improve our rupture forecasts and might also help to address the so-called "paleo hiatus" problem in California (Biasi and Scharer, 2019).

Target MFDs and b-value Branches

Solving for the rate of ruptures from slip rate and paleoseismic event rates is an inherently underdetermined problem, meaning there is a wide range of models that can fit the data equally well (the null space). We therefore need a mechanism to control where each inversion lands in this null space so we can define a representative set of viable models (epistemic uncertainty). We can achieve this by specifying a target MFD shape for each fault section, and thus far we have assumed a Gutenberg-Richter distribution and specified the target *b-value* (the slope of the distribution in log-linear space). By adjusting the *b-value* over a range of values (e.g., between 0.0 and 1.0), we effectively consider a range of total-rate models that are believed to cover an adequate range of models in terms of hazard implications (and note that the *b-value* = 0.0 case produces a system-wide MFD with *b-value* ≈ 1.0 due to varying fault sizes).

To date, applications have assumed that on-fault *b-values* are correlated across the region, which may not be correct. Adjacent fault sections most certainly have correlated *b-values* (because they participate in the same larger events), but it is also reasonable to presume that distant faults are not correlated. Assuming full correlation is more reasonable for site-specific hazard curves because they are typically influenced by just a few nearby faults. However, the assumption is more questionable for spatially distributed hazard and risk estimates (e.g., average annual statewide losses), so one might at least want to lower the weights on extreme branches. Better yet, we would define a specific *b-value* correlation structure, but unfortunately it is not obvious how to do so. Additionally, there may be certain well-studied faults (or categories of faults, such as those in a particular region and of a certain faulting style) that warrant different weighting of the *b-value*

branches. In the meantime, exploring the implications of current assumptions with respect to spatially distributed hazard and risk metrics (a work in progress) could be influential.

Segmentation Constraints

Segmentation refers to the extent to which ruptures are confined to individual faults versus being capable of jumping to neighboring faults (as multi-fault ruptures). An important recent innovation is the addition of flexible and efficient segmentation constraints that are (optionally) jump-distance dependent (Milner and Field, 2023). The degree of segmentation is quantified by the fractional passthrough rate (set to zero for strict segmentation and 1.0 for zero co-rupture penalization). This is applied as an inequality constraint, meaning relative passthrough rates can be less but not greater than the target value (depending on the influence of other inversion data constraints). For the western U.S. portion of the 2023-CONUS-ERF-TI, we defined five different logic-tree branches, going from a maximally segmented (classic) model to a completely unsegmented model (fault-to-fault jumps up to 15 km), with three intermediate models having various degrees of distance-dependent passthrough rates. Note that these branches also reflect fault model uncertainties. For example, allowing a 15 km jump is in part a proxy for an unknown connector fault being present, and preventing short jumps via the classic model can be a proxy for the connectivity being over estimated.

We believe this set is a good representation of the viable range, with the current question being whether any branches should be trimmed, or their weights adjusted. For example, there was much discussion of whether the more permissive branches are inconsistent with a lack of globally observed crustal ruptures with lengths exceeding 500 km (see text regarding Figure 21 of Field et al., 2023). To this end, detailed surface-rupture observations and statistical analyses thereof (e.g., Biasi and Wesnousky, 2016, 2017; Rodriguez Padilla et al., 2024) might be informative, but

attempts thus far have been hampered by questions like whether those details project to depth and that our fault models generally lack such detail in the first place (our simplified traces do not reflect the detail we expect in future large ruptures). Questions also remain on whether ruptures can completely pass through the San Andreas creeping section, perhaps rupturing the entire San Andreas fault; answers implied by our 2023 model range from yes to no. As with the *b-value* constraint above, we have assumed full spatial correlation with respect to segmentation branches (e.g., the classic model applies everywhere), which again may be a questionable approximation with respect to spatially distributed hazard and risk metrics. We did not find these questions highly influential with respect to 2023 NSHM results (time-independent hazard curves at individual sites), but they could be highly consequential with respect to spatially distributed hazard and risk metrics (e.g., average annual loss in California). Going forward, global compilations of observed rupture lengths and fault-jump distances will be important to further constrain both these and more physics-based models.

Implementation Details

While we have asserted that fault system solutions are conceptually simple, we also admit that the inversion-based solutions are far from trivial and will always remain a black box for many stakeholders. As such, it is important to interrogate results in every imaginable way, which we have thus far accomplished via extensive web-based solution reports (e.g., Milner and Field, 2023). So far, results have passed muster with respect to representing best available science (e.g., according to the 2023-CONUS-ERF-TI review panel; Jordan et al., 2023). Considerable effort has also gone into the computational infrastructure in terms of numerical efficiency, automatization, and reproducibility (Milner and Field, 2023). That said, the remainder of this section discusses some implementation details or features that might benefit from further refinement.

One challenge is handling correlation between the *b-value* and fault-segmentation branches because the latter has a strong influence on the MFD shape as well. A variety of solutions were explored by Milner and Field (2023), several of which worked equally well in terms of equivalent hazard implications, but it's possible that something even better could be developed.

Our focus on supra-seismogenic ruptures (full down-dip ruptures) means that the minimum magnitude on some shallow dipping faults can be as large as *M* 7 (smaller events are treated as gridded seismicity). In other words, we no longer float ruptures down dip, which could be rectified if deemed problematic (especially on subduction zones, as exemplified by Gerstenberger et al., 2024).

We continue to use simulated annealing to solve the inverse problem, but it's possible that an even better numerical solver could be found with respect to: computational efficiency; controlling where results land in the solution space; even-fitting data (getting a range of solutions that mimic data uncertainties); and generating models with smoother MFDs, minimized rate variability along strike, and better control on the fraction of zero-rate ruptures.

With respect to reducing fault slip rates by the amount taken up by subseismogenic ruptures, we have not yet found an algorithm for obtaining fault-specific values (assumptions required are highly questionable). Although the impact is generally negligible relative to overall uncertainties, further refinements here might be value added.

Adding Other Geologic Constraints

A significant enhancement for fault system solution inversions would be support for other geologic constraints, such as paleoliquefaction, tsunami inundation, fragile geologic features, or paleolacustrine disturbances or deposits, some of which are already used to constrain CEUS and

subduction-zone sources (e.g., Thompson Jobe et al., 2022; Walton et al., 2021). A challenge is that none of these observations relate directly to rupture rates, but rather reflect ground shaking events. One approach is to assume the observations only associate with ruptures on a specific fault (or fault zone), which is effectively what has been done to date. This makes sense if strict segmentation or a characteristic rupture is assumed, but the inversion approach relaxes these assumptions. In general, there will be many different ruptures that could have produced the observations, so what we ultimately need are models that provide the probability of producing the disturbance given any arbitrary rupture. Implementing such constraints in the inversion will be relatively easy compared to creating these probability models. A more modest approach would be to check hazard results against such models (post processing reality check), perhaps leading to branch weight adjustments.

Gridded Seismicity Sources

Gridded seismicity or "background" sources represent the seismicity that is not captured by explicitly modeled faults (see Llenos et al. (2024) for a recent example). These are presently composed of:

1) A polygon defining the region and a spatial discretization interval to define the grid cells (typically 0.1 degrees)
2) A spatial probability distribution defining the relative rate of earthquake nucleation within each grid cell
3) A *Total M≥5 Rate* and *b-value* for the region
4) An assumed maximum magnitude for the region (or spatial distribution thereof)

5) A probability distribution of focal mechanisms for each grid cell

6) Rules for converting a nucleation point into a finite rupture surface (usually application of a random strike)

This type of source is also used to represent events within a down going subduction slab. The main ingredients utilized in generating the above elements are an earthquake catalog, aftershock declustering algorithms, and spatial smoothing procedures.

Earthquake Catalogs

Earthquake catalogs usually represent an aggregation of events identified by seismic networks (instrumental seismicity) and those inferred from historical records (e.g., newspaper accounts). Important steps in assembling a suitable catalog (e.g., Mueller, 2019) include the removal of duplicate events (recorded by multiple seismic networks), explosions and other mining-related events, and perhaps other human-induced earthquakes (depending on how these are handled in the model). Network reported magnitudes are generally converted to uniform moment magnitudes, and bias corrections are made with respect to sampling events from a Gutenberg-Richter distribution. Ideally, uncertainties are provided for all event attributes. Finally, magnitude incompleteness estimates are needed to define the probability that events went undetected (ideally as a function of time, space, and magnitude).

Multiple issues make achieving a uniform earthquake catalog challenging. Routinely determined magnitudes are subject to numerous potential biases, which vary as a function of magnitude type, space, time, and monitoring network. Although conversion relationships have been developed in some areas to try to homogenize the available catalog magnitudes to uniform moment

magnitudes (Electric Power Research Institute/Department of Energy/Nuclear Regulatory Commission, 2012), these conversion relationships do not always perform well, and biases of up to 0.5 magnitude units (equivalent to a factor of ~3 in seismicity rate for typical *b*-values) have been observed in some cases (e.g., Shelly et al., 2022). These biases can also impact the estimated *b-values* from a catalog.

Fortunately, avenues exist to improve catalog homogeneity. Although previous work has mostly used a single "preferred" magnitude for each earthquake in the catalog, for modern events multiple magnitudes often exist, and these magnitudes could be used together to provide a more stable converted moment magnitude. Further use of techniques that can directly compute moment magnitude for small events (e.g., Mayeda et al., 2003) could also help to calibrate conversion relationships and reduce dependency on them.

Total Regional Rate and b-value Estimates

The total magnitude-frequency distribution of a region is usually assumed to follow a Gutenberg Richter distribution, which can be specified by the *Total M≥5 Rate*, *b-value*, maximum magnitude, and the shape of the distribution at the largest magnitudes. State of the art for inferring *b-value* is the "b-Positive" technique of van der Elst (2021). Inferring *Total M≥5 Rate* is less standardized, often involving Monte Carlo sampling algorithms that account for uncertainties in *b-value*, event magnitudes, and spatially and temporally variable magnitudes of completeness. A particular concern is whether such procedures produced biased estimates in low-seismicity regions (Iturrieta et al., 2024).

Gridded Seismicity Spatial PDFs

Inferring the long-term spatial probability density function of seismicity rates requires catalog declustering. Otherwise, rates will be biased high where larger events happen to have occurred and biased low where they have not (e.g., Frankel, 1995). Lacking a perfect model for aftershock occurrence, a variety of catalog declustering algorithms have been adopted, including Gardner and Knopoff (1974), Reasenberg (1985), Zaliapin and Ben-Zion (2020), and others. Declustered catalogs are then smoothed and normalized to provide a spatial probability distribution of event nucleation, typically using either a fixed width, two-dimensional (2D) Gaussian kernel (Frankel, 1995) or an adaptive-width, nearest-neighbor algorithm that provides a more spatially refined estimate where there is a higher density of observed events (Helmstetter et al., 2007). Floor-level rates may be applied in areas with very few earthquakes. See Llenos et al. (2024) for recent examples of these procedures, and Llenos and Michael (2020) for a newer, promising approach that is particularly attractive in terms of being more consistent with assumptions made in the fully time dependent models discussed below.

A large uncertainty that has yet to be fully addressed is the sampling error associated with this spatial distribution being inferred from one historical sample of earthquakes. In other words, is what we have inferred from recent history consistent with what we may see in the next equivalent timeframe, or what is the variance we should see over 10,000 such samples? The fully time-dependent models discussed below (including spatiotemporal clustering) are seemingly required to adequately address this question, as they can provide any number of historically consistent samples with realistic aftershocks sequences. However, we will need to operationalize these analyses, and perhaps utilize high-performance computing, to handle such large synthetic data sets.

Maximum Magnitudes, Focal Mechanisms, and Finite Rupture Surfaces

Assumptions regarding maximum magnitudes are generally based on expert opinion, in part because they are generally not that consequential, especially in areas dominated by fault-based ruptures. Nevertheless, further investigations could be impactful, especially for longer period ground motions in seismically quieter regions. Promising approaches include pooling data across tectonically similar regions (Coppersmith et al., 2012; Vanneste et al., 2016) and extreme value theory (although Zöller (2013, 2022) articulates challenges with the latter).

The spatial distribution of focal-mechanism probabilities is another area of potential improvement. Current models generally specify the fraction of strike slip, reverse, and normal faulting events over large regions, and assuming a uniform probability of strike direction, so we could certainly do better by considering regional stresses, earthquake focal mechanisms, and geologic fabrics. Whether this would be value added in terms of hazard assessment remains to be seen.

A related issue is how to turn a nucleation point into a finite rupture surface, with a number of approximate procedures currently being available. Although these details may not be hugely consequential either, improvements may be desired from an elegance perspective as we produce synthetic catalogs from fully time-dependent models (discussed below). For example, are we willing to tolerate a gridded seismicity event that has a rupture surface crossing an explicitly modeled fault (such as the San Andreas)?

Merging Fault and Gridded Seismicity Source Models

The MFD defined for gridded seismicity represents the regional total, including fault-based sources, so it can be important to avoid double counting. This is now typically done by subtracting the fault-based MFD from the regional total and applying the result to gridded seismicity, with

perhaps additional care in terms of tapering the rate of large, gridded-seismicity events in the vicinity of fault-based sources. Although the latter is not very consequential in terms of implied hazard, it can be an important requirement in terms getting fully time-dependent models to behave properly. No such corrections were made in the CEUS portion of the 2023 NSHM, leading to an apparent factor of ~3 over-prediction of rates at $M \geq 7.5$ (see Figure 25a of Field et al., 2023).

Earthquake Probability Models

A probability model gives the occurrence probability for each rupture (defined in the earthquake-rate model) for a specified timespan and conditioned on whatever other information is available. As such, a probability model represents a fully specified ERF. For time-independent ERFs the Poisson model is applied, as in all previous USGS NSHMs. Various time-dependent enhancements are described below, including fully time-dependent models that include spatiotemporal clustering. The latter produce synthetic catalogs (stochastic event sets) from which rupture probabilities can be inferred.

Long-Term Time Dependence - Elastic Rebound

The most common type of time-dependence is elastic rebound, where the probability of a large event drops where and when a fault has had a large rupture and grows with time as tectonic stresses reload (Reid, 1910). A classic renewal model (e.g., Lognormal or Brownian Passage Time) is usually used to represent the recurrence-interval distribution. The procedure becomes non-trivial once a strict fault-segmentation assumption is relaxed, as overlapping adjacent ruptures can produce short recurrence intervals at points on faults, which are generally inconsistent with the

851 renewal model being assumed (and perhaps biasing probability estimates as well). A solution to
852 this problem was developed for the UCERF3 long-term time-dependent model (Field et al., 2015),
853 based in large part on studying results from multi-cycle physics-based-simulators (Field, 2015).
854 Additional benefits of this algorithm include probability estimates even where the date of last event
855 is unknown and the option for magnitude-dependent coefficients of variation (less periodicity for
856 smaller ruptures). This algorithm remains best available science, as we know of no viable
857 alternatives at this point. The algorithm is far from perfect, however. For example, perhaps
858 coefficients of variation should also depend on fault maturity (more periodicity on well-worn or
859 higher slip-rate faults?). With any such algorithm, it is important to verify that Monte Carlo
860 simulations (randomly sampled earthquakes over long time periods) produce rates that are
861 consistent with what is assumed in the first place.

862

863 **Short-term Time Dependence - Spatiotemporal Clustering**
864

865 Spatiotemporal clustering (aftershocks and otherwise triggered events) is the other obvious
866 time dependence to include. In fact, previous USGS NSHMs have included "cluster" models where,
867 for example, in the latest model some large New Madrid, Missouri earthquakes are assumed to
868 occur as doublets or triplets, and there is an option where a series of *M* 8 events progress down the
869 Cascadia subduction zone. There are no statements about how quickly such events occur, other
870 than within the 50-year forecast window, so it is not clear how to apply these models in short-term
871 forecasts.

872 The Epidemic Type Aftershock Sequence Model (ETAS, Ogata, 1988, 1998) appears to be the
873 best option for representing spatiotemporal clustering, at least for now (discussed below). The

874 significant challenge is merging this point-process model with a forecast that includes finite faults.
875 The UCERF3-ETAS model (Field et al., 2017) represents one attempt to do so, raising several first-
876 order questions and issues:

877

878 • What is the long-term MFD near faults, and how does this transition spatially into the
879 surrounding region?

880 • An elastic-rebound component is apparently needed to suppress re-rupture of the same
881 fault surface (without it, a triggered event will spatially overlap with the triggering
882 event much more than is seen in nature).

883 • Can a large, triggered event nucleate from well within the rupture area of the triggering
884 earthquake? (this has a first order influence of conditional triggering probabilities in
885 UCERF3-ETAS)

886 • For implied long-term rates to match those defined in the earthquake rate model, one
887 needs a time-dependent fraction of spontaneous (versus triggered) events due to our
888 limited knowledge of previous earthquakes, and spatial variability as well in areas
889 where MFDs are non Gutenberg Richter.

890

891 So far UCERF3-ETAS appears to produce realistic and plausible results (Page and van der Elst,
892 2018), as illustrated in **Figure 3**. However, it embodies a host of assumptions and approximations,
893 and the implications of many uncertainties have yet to be thoroughly explored. The important
894 point here is that there is lots of room for potential improvements. One particular challenge is
895 having rates implied by very long-duration simulations exactly match those implied by the
896 underlying long-term model; in fact, this may never be possible, but these discrepancies should at

least be significantly less than overall epistemic uncertainties. Another challenge is representing epistemic uncertainties, especially because they can evolve with time (e.g., aftershock productivity estimates) and the ballooning number of branches. Improving these models, not to mention deploying them as operational earthquake forecasts (discussed below), might require significant resources. We may also need to enlist multi-cycle physics-based simulators to address many of the questions posed here.

Induced Seismicity

Induced seismicity refers to earthquakes caused by human activities, such as those associated with oil and gas extraction, geothermal energy, and carbon dioxide sequestration (e.g., Ellsworth, 2013). Cochran et al. (2024) provide a comprehensive overview and strategic vision with respect to USGS efforts in this area, including state of knowledge, research activities, and efforts to quantify associated hazards. Following an alarming increase in seismicity rates caused by expanded oil and gas operations in the central United States between 2009 and 2015, three 1-year induced seismicity forecasts were published by the USGS NSHM (Petersen et al., 2016, 2017, and 2018). These "official" forecasts have so far been based on a pure gridded seismicity model (described above), with particular challenges being catalog quality, distinguishing induced from tectonic events, what type of declustering is appropriate (if any), how to extrapolate low-magnitude *b-values* to higher magnitudes, and whether the maximum magnitude of induced earthquakes should be the same as that assumed for tectonic events. Updates for such USGS induced-seismicity forecasts are on hiatus because seismicity rates are no longer increasing in Oklahoma (for now), other competing priorities and limited resources, addressing important questions related to declustering, and taking a strategic pause to gauge actual uptake in user communities.

More complex models have also been explored, such as ETAS with a time-varying rate of spontaneous events (Llenos and Michael, 2013), and more physics-based approaches that combine stressing rate changes from injection with rate-and-state-based friction models (e.g., Norbeck and Rubinstein, 2018; Rubinstein et al., 2021). See Cochran et al. (2024) for other examples.

Going forward, it could be beneficial to ensure that development of these models is well coordinated and integrated with other ERF developments, and that computational resources are shared as much as possible. For example, if we succeed in operationalizing statistical seismology processing for the gridded seismicity components, short-term forecast updates might become relatively effortless.

Static Stress Change Models

The 1992 Landers earthquake and a 70-year sequence of events on the North Anatolian fault implied that static stress change models might be useful in forecasting large, triggered events (e.g., King et al., 1994; Stein et al., 1997; Parsons and Dreger, 2000). This approach computes the spatial distribution of stress change caused by a main shock and applies the rate and state model of Dieterich (1994) to infer event probabilities. Although there was hope this might "dramatically improve scientists' ability to pinpoint future shocks" (from the sub-title of Stein (2003)), the ultimate value remains to be seen, as Coulomb rate-and-state models rarely outperform statistical models such as ETAS (Woessner et al., 2011; Segou et al., 2013; Catannia et al., 2018). However, Mancini et al. (2020) found that physics-based models outperform ETAS for the Ridgecrest earthquake, with accounting for faulting heterogeneities and secondary triggering being critical to success. Furthermore, our assertion above that elastic rebound is needed to get spatiotemporal

clustering models to work with finite faults suggests that some relaxation process exists, implying there is something to static stress change. Parsons et al. (2023) tested this prospectively following the 2008 *M* 7.9 Wenchuan earthquake in China; as of 2023, all but one of the subsequent shocks in the region that caused casualties were identified as posing increased hazard in 2008, and the exception was triggered by induced hydraulic fracturing. Remaining questions include: 1) defining fault orientations of potentially triggered events; 2) the competing influence of dynamic triggering effects (e.g., Parsons, 2002; Hardebeck and Harris, 2022); and 3) the extent to which we can resolve stress-change distributions given uncertainties in mainshock slip and crustal heterogeneities, which appears to cause an underestimation of the observed degree of spatial clustering (Hardebeck, 2021). Furthermore, we need to run such models over multiple cycles to ensure there are no systematic biases; doing so would make such models consistent with the multi-cycle physics-based simulators described below.

A final application of static stress transfer concepts can be applied to the whole crust by using fault-based earthquake rate models to calculate the long-term stress effects of slipping the model in the surrounding crust. If we find large positive stress concentrations in regions where there are no mapped faults, we may be missing seismic sources and/or the result can be compared with observed background (off-fault) seismicity as a means of model testing.

Machine Learning Approaches

In recent years, multiple research groups have made progress in applying machine-learning models to the temporal (Dascher-Cousineau et al., 2023; Stockman et al., 2023) and spatiotemporal earthquake forecasting problem (Zlydenko et al., 2023). Future earthquake rates can be forecast

using a neural point process (NPP) trained on past seismicity, and, with enough training data, these machine-learning-based methods outperform simple ETAS formulations (Dascher-Cousineau et al., 2023; Stockman et al., 2023; Zlydenko et al., 2023). Machine-learning formulations have the advantage of being extremely flexible: they can quickly adapt to the productivity of an ongoing aftershock sequence; they infer non-stationarities and irregularities present in earthquake catalogs; and they continue to improve with additional small earthquakes, even if catalogs are highly incomplete (e.g., Stockman et al., 2023). Some models can also be used to make multiple synthetic catalog continuations, much like ETAS (Dascher-Cousineau et al., 2023). NPP models also require significantly less computational power to train for large datasets compared to ETAS, since they scale linearly with the number of training earthquakes rather than quadratically (Dascher-Cousineau et al., 2023). There are challenges, however, like whether these models can produce long synthetic catalog continuations that remain accurate, and how they perform with respect to the larger (and rarer) events that influence seismic hazard.

Other Time Dependencies

Real earthquakes almost certainly embody other time dependencies, with one obvious example being earthquake swarms, which represent sequences of seismic events that occur in a localized area over a short period of time without a single outstanding mainshock. Unlike typical earthquake sequences, which have a clear mainshock followed by smaller aftershocks, swarms consist of numerous earthquakes of similar magnitudes. Swarms can last from days to years and are often associated with volcanic or geothermal activity, although they can also occur in tectonic regions. The causes of earthquake swarms are diverse, including magma movement, fluid injection or extraction, and tectonic stress adjustments. Efforts to model such events for hazard quantification purposes include Llenos and Michael (2019) and Llenos and van der Elst (2019).

Other time dependencies are implied by the "paleo hiatus" discrepancy identified by David Jackson (Biasi and Scharer, 2019), “super cycles” , which refer to clusters of large events that are separated by some period of time (Grant and Sieh, 1994; Weldon et al., 2004; Dolan et al., 2007; Goldfinger et al., 2013; Rockwell et al., 2014; Schwartz et al., 2014), and “mode switching”, which represents the idea that one region or fault will activate for a time and then shut down as another area activates (Dahmen et al., 1998; Ben-Zion et al., 1999; Zaliapin et al., 2003; Ben-Zion, 2008, Hatem and Dolan, 2018). Another is apparent seismicity rate changes associated with strain accumulation over seismic cycles (e.g., Zeng et al., 2018) and temporal changes in fault slip rates (e.g., Wallace, 1987). Current official probability models also lack the ability for a long rupture on one fault to temporarily reduce the likelihood of such an event on an adjacent nearby fault (e.g., the 1906 SAF earthquake stress shadowing the parallel Maacama fault, which is something static stress models could account for). The practical question is whether these effects are significant with respect to inferred hazard and risk. Multi-cycle, physics-based simulators seem to be our best hope for addressing such questions.

Multi-Cycle Physics-Based Simulators

Multi-cycle physics-based simulators, as described in a special issue of Seismological Research Letters (Tullis, 2012), are arguably our best hope for addressing many earthquake-forecasting questions, especially given the slow trickle of large-event observations. Rather than the traditional approach of inferring earthquake magnitudes from fault area or length using statistical scaling relationships, and associated frequencies of occurrence by matching fault slip-rate and/or paleoseismic recurrence intervals, these physics-based models apply tectonic loading to a fault system and utilize frictional properties on those faults to determine when and where earthquakes

occur, with each earthquake transferring stress and thereby influencing the occurrence of subsequent events. This approach effectively combines the earthquake rate and probability components (**Figure 4**), and the output is a synthetic catalog of earthquakes covering thousands to millions of years (or whatever is desired).

Common Criticisms

All models embody assumptions, approximations, and input-data uncertainties, so the relevant question is whether such simulators are useful. A common criticism is that there is not yet enough physics in the current physics-based simulators. But enough physics for what? The potential usefulness of a model cannot be ascertained outside the context of a specific inference, and answers will certainly vary among different uses (i.e., inferring elastic rebound predictability versus inferring the propensity of multi-fault ruptures). And even if we get the physics and numerical approximations exactly right, we will still be plagued by uncertainties in what faults look like at depth (e.g., Zielke and Mai, 2025). We therefore should not let perfection be the enemy of a more useful model.

That said, significant challenges remain with respect to these models. Perhaps the most pressing is that they generally ignore, or crudely approximate, the influence of propagating seismic waves (inertial/dynamic effects). They also generally ignore the 3D velocity structure, non-elastic effects at depth, off-fault yielding, and other things such as the influence of fluids. Single-cycle (single-event) dynamic rupture models (e.g., Harris et al., 2018) are better able to represent such effects, but computational limits currently limit such sophistication in the multi-cycle models needed for earthquake forecasting. The relevant question is their relative value in the context of implied epistemic uncertainties and the cost of development and maintenance.

The ultimate inference would be the probability of future ruptures, conditioned on what we know about past events. However, we cannot simply start these models at present conditions and get multiple realizations of what comes next. This is because they must be "spun up" for thousands of virtual years before stable behavior emerges, leaving one to search for periods in a simulation that match as close as possible to the historical record (e.g., Aalsburg et al., 2010). In other words, even if these models were a perfect representation of nature, there would still be work in terms of figuring out how to use them to infer time-dependent earthquake probabilities.

Potential Inferences

A more modest use of multi-cycle physics-based simulators is to test various implications, assumptions, or epistemic uncertainties in current ERFs, such as those associated with:

- Average rupture rates
- Multi-fault rupture plausibility (Milner et al., 2022)
- Scaling relationships
- Average slip along rupture, especially for multi-fault events
- MFDs near faults (non Gutenberg Richter?)
- Influence of creep (area versus slip-rate reduction) and seismogenic depths
- Elastic rebound predictability (e.g., Field et al., 2015)
- Spatiotemporal clustering (e.g., is ETAS adequate at large magnitudes?)
- Other time dependencies (mode switching, super cycles, paleo hiatus)

These multicycle simulators may also represent our best physics-based option for obtaining multiple slip-time-history realizations for specific ruptures, which are needed to address ground-motion questions such non-ergodic effects and how directivity manifests for multifault ruptures.

Currently Viable Models

Multi-cycle simulators have been around for decades and continue to be improved upon. Here, we focus on current models that can accommodate the space and time scales that interest us, meaning hundreds of faults and thousands of years. This means approximations must be made, including the abandonment of inertial waves (analogous to climate versus weather models). Smaller scale tests should be conducted against more sophisticated models to ensure consistency (e.g., Harris, et al, 2009; Jiang, et al, 2022; Erickson, et al, 2023), although comparisons will eventually need to be statistical in nature given the effective stochasticity of results (Tullis, et al, 2012).

Given overall limitations, it would be advantageous to have a wide variety of simulators under development and analysis, both for epistemic uncertainty quantification and ensemble forecasting. Although the following reflects the currently limited number of models (that we know of), hopefully this discussion will motivate other efforts.

RSQSim

RSQSim stands for "**R**ate and **S**tate Earth**Q**uake **Sim**ulator" (Dieterich and Richards-Dinger, 2010; Richards-Dinger and Dieterich, 2012; Shaw, 2019). It models a complex fault system using

rectangular or triangular boundary elements with back slip. It avoids repeated incremental solutions of large system of equations by applying event-driven computations based on changes in fault sliding state, where each element may be in only one of three sliding states: 1) locked (aging by log time of stationary contact); 2) nucleating slip (analytic solutions of the rate-state equations for accelerating slip to nucleate earthquakes, and track the time- and slip-dependent breakdown process at the rupture front); and 3) earthquake slip (quasi-dynamic, in which slip speed is based on shear wave impedance). The model is thereby currently able to model millions of years of M≥4 earthquakes throughout a large complex fault system. RSQSim can also model slow-slip events, fault creep, induced seismicity, and the interaction of these with normal tectonic events. Comparisons with fully dynamic, finite-element simulation for individual ruptures (Richards-Dinger and Dieterich, 2012) show good agreement, and rupture jumps between disconnected faults are in good agreement with more detailed rupture modeling. RSQSim also produces realistic spatiotemporal clustering (aftershocks or Omori behavior) as inferred from interevent waiting time distributions and space-time distributions.

RSQSim has already contributed to earthquake hazard estimates, including elastic rebound inferences (Field, 2015), scaling relationships (Shaw, 2023), developing improved rupture sets for fault inversions (Milner, et al, 2022), and fault segmentation parameterizations (Milner and Field 2023). It has also been shown to replicate long-term hazard at the scale of fault systems (Shaw, et al, 2018). As such, RSQSim remains a leading simulator based on capabilities, validation, and applications to hazard.

MCQsim (Zielke and Mai, 2023)

MCQsim stands for "**M**ulti**C**ycle Earth**Q**uake s**im**ulator". Like RSQSim, it uses triangular boundary elements that interact elasto-statically to create cascading earthquake ruptures (as well

as inter- and post-seismic phases) on arbitrarily complex fault geometries. In contrast to RSQSim, MCQsim uses a linear slip-weaking law to describe frictional breakdown during sliding. Fault elements exhibit unstable, conditionally stable or stable seismogenic behavior, based on their strength relative to elastic properties of the half-space and their slip-weaking distance. As such, the MCQsim natively provides an upper and lower depth for the seismogenic zone, further permitting incorporation of strength asperities, fault after-slip, and partial locking (i.e., creep). Coseismic slip rates are limited by a radiation damping approximation that is continuously updated during the rupture phase. Yoffe-like slip pulses, similar to those in dynamic rupture simulations, emerge from the simulations. A nice feature of the model is that it optionally includes plastic loading on the lower crust, with stresses relaxing postseismically on the lower horizontal surface below the seismic faults, in a Maxwellian exponential decay. While there is not a nucleation process that would lead to Omori-law clustering, the viscous relaxation process (also present as after-slip on conditionally stable and stable elements) does enable some longer time scale and finite depth crust interactions to be explored. A comparison of an individual rupture starting from the same initial conditions against an elastodynamic finite element code and RSQsim (Richards-Dinger and Dieterich, 2012) shows good correspondence between all three models (Zielke and Mai, 2023). The ability of the model to simulate complex, individual ruptures and complex sequences of ruptures on complex fault networks with a range of geometries and rakes makes this a promising model. MCQsim model development is ongoing (e.g., implementation of H-matrices, poro-elastic effects, alternative tectonic loading, topography, and layered medium) to further boost its capabilities, computational efficiency, and applicability to earthquake forecasting.

Tandem (Uphoff et al., 2022)

Tandem is an open-source software package for the simulation of earthquake sequences and aseismic slip in volumetric domains accounting for complicated geometries (e.g., topography, complex fault systems) and heterogeneous subsurface properties. It is the first muti-cycle earthquake simulator to use the Discontinuous Galerkin differential equation solver, and it utilizes the Portable, Extensible Toolkit for Scientific Computation (PETSc, Balay et al., 2023) for scaling and parallelization on a wide variety of advanced high-performance computing platforms. The model supports both quasi-dynamic and fully dynamic rate-and-state friction capabilities, although the extent to which the latter can scale to large fault systems remains to be seen. It can handle complex curvilinear, intersecting faults and inhomogeneous bulk material properties. It has demonstrated good agreement with other codes in community benchmark problems (Uphoff, et al., 2022, Erickson et al., 2023) and in applications (e.g., Biemiller et al., 2024). In recent work, Tandem has been utilized to simulate seismic cycles in subduction zone settings, introducing curved megathrust geometries and variations in elastic parameters dependent on distance from the trench and depth (Biemiller et al., 2024). These variations can significantly influence the behavior of earthquake cycles. These simulations help to more comprehensively understand how co-seismic, post-seismic, and inter-seismic deformation interact across multiple earthquake cycles.

A Path Forward

Confidence in inferences would certainly be bolstered by consistency among several alternative simulator models. The reality is, however, that these models are challenging and expensive to develop and maintain, as they typically require collaboration with computer scientists, access to high-performance computing, an ability to curate and document both computer codes and results, and an ability to reproduce the latter. They also depend on inputs that are themselves difficult to develop and maintain (e.g., detailed fault models).

With respect to not having "enough" physics, we need to define smaller-scale test problems so they can be compared against more sophisticated methodologies (e.g., full dynamic models). To this end, it would be beneficial to have a set of standard evaluation metrics, including whatever inferences are desired with respect to ERF development (e.g., the list above). Again, we will have greater confidence to the extent that alternative models agree with respect to inferences. For example, we already noted that our elastic-rebound predictability algorithm was inferred from a number of simulators, so the challenge now is whether a viable simulator can be constructed that does not exhibit such behavior. Even if all current models are found lacking in terms of usefulness, it only means we may need to push development even harder, especially if they are really our best hope for improved ERFs. That said, these models will always be an approximation of the system, especially with respect to limited knowledge of subsurface structural details, so inferences will need to be considered carefully on a case-by-case basis.

Operational Earthquake Forecasting (OEF)

Operational Earthquake Forecasting (OEF) aims to provide authoritative, real-time information on evolving earthquake probabilities, including triggered events (Jordan and Jones, 2010; Jordan et al., 2011). While it is one thing to develop a fully time-dependent ERF (described above), it is quite another to deploy it as a continuously running, real-time system.

The USGS has been issuing various aftershock warnings since the 1980s, providing the probability of aftershocks above various magnitude thresholds (Roeloffs and Goltz, 2017). Significant progress has been made in recent years with respect to updating computer codes to a modern modular framework, defining region-dependent generic parameters, implementing sequence-specific parameter estimation (especially for productivity), improving how real-time

1176 catalog incompleteness is handled, implementing an automatic forecasting system, having a manual
1177 graphic-user-interfaced-based application for both computing and pushing results to USGS web
1178 pages, implementing a tiered-communications strategy with both graphics and text, and versioning
1179 results for posterity and testing purposes. Many of these capabilities were exemplified by Michael
1180 et al. (2019).

1181 Progress is also being made with respect to replacing the traditional Reasenberg and Jones
1182 (1989, 1994) algorithm with an ETAS model because it handles large aftershocks more elegantly
1183 and can more easily provide the spatial distribution of expected aftershocks. Adopting an object-
1184 oriented framework has made this transition from Reasenberg-Jones to ETAS much easier (plug
1185 and play with respect to most downstream analyses), and use of *OpenSHA* (Field et al., 2003) has
1186 made the generation of hazard curves and maps relatively easy. To make this work effective, user
1187 workshops held in the United States, Mexico, and El Salvador focused on understanding user needs
1188 and improving communications of aftershock forecasts and short-term hazard maps (Schneider et
1189 al., 2025).

1190 These aftershock warnings are called Operational Aftershock Forecasting (OAF) because they
1191 address only triggered events. OEF, on the other hand, aims to forecast all events (spontaneous and
1192 triggered), with the model of Gerstenberger et al. (2004) being a pioneering example, and Spassiani
1193 et al. (2023) being a more modern (ETAS) example. The primary advantage of OEF, versus OAF, is
1194 the ability to quantify probability gains with respect long-term or pre-mainshock values (e.g., see
1195 Field et al. (2018) for various hazard and risk examples for the "Haywired" scenario based on
1196 UCERF3-ETAS and a no-faults version of the model). In contrast to OAF's event-triggered mode of
1197 operation, OEF could be run at any or all times, enabling users to define actionable thresholds
1198 themselves (honoring the hazard-risk separation principle; Jordan et al., 2014) or to know when
1199 probabilities are unusually low.

A series of USGS Powell Center workshops were conducted between 2015 and 2018 to review best-available science and potential usefulness of OEF, with a number of stakeholders and likely early adopters in attendance (e.g., Field et al., 2016). In short, OEF was deemed potentially useful in that probability gains can far exceed the 10% actionable threshold typically defined by users, but legitimate questions remain with respect to the influence of temporal decay and delays in issuing forecasts (latency). Based on the outcome of the Powell Center meetings, together with a follow up review of viable models, the National Earthquake Prediction Evaluation Counsel (NEPEC) wrote the following in a 2017 report to the USGS Earthquake Hazards Program:

> *"…the Council strongly recommends that the USGS press forward to develop a fully operationalized nationwide OEF system that carries calculations, combining the background rate of seismicity and earthquake clustering, through to hazard."*
>
> (see **Data and Resources** section for a link).

Development of OEF has been hampered in part by information technology (IT) requirements (not just more resources, but also better coordination of the ones we have). There is also the question related to operationalization. UCERF3-ETAS can be run by a human on demand, as demonstrated following the Ridgecrest sequence (Milner et al., 2020; Savran et al., 2020). Automating the system would require a significant increase in effort, which requires ensuring that the value of doing so would outweigh the costs. Here we have a bit of the chicken-and-egg problem (users cannot deem it useful without having access to such a model, and we don't want to deploy the model unless it is useful). The solution appears to be an iterative one, in which fully time-

dependent (but non-operationalized) results are made available so that users can explore various "what if" questions. Given that the risk modeling community stands to benefit particularly from such models, it would also help to calculate various risk metric during the model-building process (in-house valuation). This would allow knowing whether the latest NSHM is appropriate for shorter-term and spatially distributed hazard and risk metrics.

Model Testing and Valuation

Model testing is both a hallmark of science and critical for any predictive models used by society. As noted, the paucity of large event data makes testing earthquake forecasts particularly challenging. Furthermore, human frailties like apophenia (seeing signal in noise) and confirmation bias (ignoring contrary evidence) imply that an independent, objective process of evaluation is needed. Our primary solution to this has been the Collaboratory for the Study of Earthquake Predictability (CSEP; see **Data and Resources**), which represents an infrastructure for testing earthquake forecast models. This international effort has produced interesting results (e.g., see Michael and Werner (2018), which is the preface to a CSEP-related special issue of Seismological Research Letters), including the conclusion that ETAS remains the best model with respect to spatiotemporal clustering, but that more physics-based and machine-learning approaches may be catching up. However, these tests only have strength at lower magnitudes, and our ability to test models at the large magnitudes that dominate hazard ($M \geq 6.5$) continues to be hampered by the limited large-event observations, which may always be the case. Nevertheless, successful testing at lower magnitudes is still useful if such events are used to forecast the occurrence of larger ones (as in ETAS), making passing these tests a necessary (but not sufficient) condition. Another approach is to put candidate models through a standard battery of “Turing tests” (e.g., the Page and van der Elst

(2018) evaluation of UCERF3-ETAS). These included evaluating total regional rate variability, the spatial distribution of aftershocks, the mean and variability of aftershock productivity, the depth distribution of earthquakes, and the nearest-neighbor analysis of Zaliapin et al. (2008). Making such analyses routine and automated would make the model development process more efficient. Finally, it is also useful to test individual assumptions or components utilized in an ERF (e.g., elastic-rebound predictability), which falls under the purview of traditional analysis and publication.

At the same time, we know all models are ultimately wrong, so what seems equally important is testing relative model usefulness, or the practical value of one model versus another (valuation). For example, it's been clearly demonstrated that aftershock productivity for a given mainshock magnitude can vary by more than an order of magnitude, and that sequence-specific models have superior forecasting skill (e.g., Page et al, 2016). However, it takes time and effort to infer sequence specific parameters, during which the sequence will have decayed to a lower level, so it is not clear that sequence-specific forecasts will always provide added value. Likewise, while UCERF3-ETAS seems to be the most realistic OEF candidate in terms of including faults, it also requires more computing power to operate. If UCERF3-ETAS and a no-faults ETAS model produce the same result for some hazard or risk metric, then why not go with the more efficient option? In other words, testing relative model usefulness (valuation) seems just as important as validation, and perhaps more so in terms of providing immediate answers that can help the USGS set deployment and scientific priorities.

The question of relative value for different options arises constantly in the model development process. We have thus far conducted such sensitivity analyses using long-term, individual-site hazard curves (i.e., building code metrics). However, as noted in the Introduction and elsewhere in this paper, such results are not necessarily applicable to other risk metrics of interest, such as

average annual loss in a region, or the loss that has a specified probability of exceedance. Consequently, some users, including one of the largest providers of homeowner earthquake insurance in the world, are currently advised to use caution with our latest NSHM (Petersen et al., 2023; Field et al., 2023; Jordan et al., 2023). The obvious solution, in addition to developing fully time dependent models, is to enable routine evaluation of a standard set of risk metrics during model development, a capability we are presently pursuing. The primary aim is to have risk results available during model development and review.

Computational Infrastructure

Comments here apply to the entire forecasting infrastructure, not just ERF development. Being able to understand and modify elements of the computational infrastructure is critical if you want to make significant forecasting improvements (as opposed to routine implementations). To this end, the following are important guiding principles:

- The infrastructure must be modular (object oriented) to allow different groups to focus on their components of interest (without having to understand details of others).
- The infrastructure needs to be accessible to scientists (the domain experts) or progress on innovations will grind to a halt; this means keeping the framework conceptually intuitive and avoiding arcane and cryptic coding options as much as possible.
- The infrastructure requires careful coordination and collaboration. Adding new features or capabilities does not always necessitate hiring an additional person (and doing so can actually impede progress).

- Robustness with respect to personnel departures (which can run counter to employee job security consideration in terms of making oneself indispensable). A related issue is having stable, long-term support.
- Access to affordable high-performance computing, especially with respect to epistemic uncertainty quantification, full time-dependent ERFs, and more physics-based models.
- Expanded support for the following types of hazard calculations: fault displacement, liquefaction, landslides, and fragile geologic features.
- Support for command-line and GUI-based apps (for those that are coding averse)
- 3D visualization capabilities

Review Process

As ERFs become increasingly sophisticated, and beyond the comprehension of any one individual, model review becomes more and more important, especially with respect to ensuring consistency among assumptions made in different model components. To this end, we will strive to maintain the formal ERF review panel established for the 2023 model (the chair of which also serves on the NSHMP steering committee). Not only did this professionally diverse group provide one of the most extensive ERF reviews to date, but they also published their findings in a peer reviewed journal (Jordan et al., 2023) -- a hugely valuable resource that influenced this document greatly. Starting this ongoing review process early, and in the context of developing a more continuous "living" research model, could help lessen the time crunch associated with building code deadlines (the next one being 2029). To keep the review process independent, membership decisions could remain under the purview of USGS Earthquake Hazards Program leadership.

We will, of course, also endeavor to host public workshops with scientists and stakeholders, as well as convene *ad hoc* groups to focus on specific elements of concern (i.e., deformation models and multi-fault ruptures for the 2023 model). Finally, we could also continue to benefit from feedback from early adopters, especially practitioners implementing the model in their own codes (which has consistently represented an important code verification process).

Discussion

The first section here reiterates and summarizes our main future objectives with respect to ERF development, and the second section gives a summary of our short-term roadmap giving steps and goals that could be achieved before the next building-code deadline in 2029. In terms of whether main future objectives are foundational versus aspirational, a theme of USGS Earthquake Hazards Program Decadal Science Strategy (Hayes et al., 2024), the answer is both; each activity is already partially funded, seemingly critical to the core functionality and global leadership of the EHP, and perhaps in need of additional support to be fully realized.

Main Future Objectives

Develop full time-dependent models (with spatiotemporal clustering)

This represents perhaps the biggest potential improvement with respect to ERFs, particularly in terms of short-term hazard and risk metrics. (e.g., insurance products), but also with respect to response and recovery efforts and performance-based engineering. For example, practitioners

generally find 10% changes in statewide average annual losses actionable (e.g., triggering an adjustment of reinsurance levels), but this metric can easily increase by an order of magnitude following a large mainshock, implying there is significant remaining predictability in the system (Field et al., 2017). Such models are also seemingly needed to, for example, address the adequacy of the Poisson assumption with other hazard and risk metrics, and to quantify historical seismicity sampling errors. The continued development of these models is therefore foundational, but their operationalization is aspirational given additional resources would almost certainly be needed.

Improved epistemic uncertainty representation

As mentioned throughout this manuscript, representing epistemic uncertainties will remain a perennial challenge (both foundational and aspirational). This includes those related to 3D fault geometries, slip rates (deformation models), the fact that we infer gridded seismicity rates from a single historical sample of events, and the degree to which epistemic uncertainties are spatially correlated. Any of these could significantly impact spatially distributed hazard and risk metrics. We also want more uniform treatments across regions, especially to avoid the paradoxical situation where fewer data constraints imply less model uncertainty. Questions also remain on how to most efficiently manage the ballooning number branches when computing hazard and risk (e.g., traverse the entire logic tree systematically, resort to Monte Carlo sampling, or hybrid approaches?), what down-sampling strategies might be appropriate for different applications, and how to best communicate these uncertainties to users.

Risk related valuation metrics

Previous USGS NSHMs have effectively been tailored for building codes (long-term, individual-site hazard curves), raising questions with respect to appropriateness for other applications (e.g., shorter-term and/or spatially distributed hazard and risk). We therefore might want to add the evaluation of risk metrics to our model-building process, which in turn will require adopting some benchmark exposure and vulnerability models (the elements needed for risk analysis, representing the distribution and value of assets and the vulnerability of each to ground shaking). There is, of course, an effective infinite number of risk metrics of potential interest, so we would need to work with users to define a minimal, necessary, and sufficient set.

Multi-cycle physics-based simulators

These models represent perhaps our best opportunity for longer-term ERF improvements, especially in terms of dealing with the lack of observations at larger magnitude. However, they also raise significant challenges with respect to model development, maintenance, and epistemic uncertainty representation. Their usefulness will also be limited by their sensitivity to rheologic and structural details that may never be well known. Nevertheless, we have already utilized these models to inform ERF development, and we will certainly continue to strive to do so. The USGS will likely continue to rely on external partners given limited internal capabilities.

Short-term Roadmap Summary

Here we outline some anticipated steps and goals we will strive to accomplish before the next building-code deadline in 2029, in approximate chronological order (and to likely begin within the next year). Results would be published and incorporated into research models as they become available. Whether versions of this living model will be sanctioned for official use will presumably be a joint decision among the authors, the review panel, and USGS earthquake hazards program

leadership. Our aims at model simplification, automated processing, and maintaining an elegant and efficient computational infrastructure should be taken as given.

Develop ERFs for U.S. territories

These include one for Puerto Rico and the U.S. Virgin Islands, Guam, and American Samoa. Anticipated innovations here include applying the inversion fault-system-solution approach to subduction zones (as exemplified by Gerstenberger et al., 2024) and dealing with earthquake catalog quality issues (e.g., biases and uncertainties).

Publish nationwide long-term time-dependent ERF

This is to account for the time-since last event on explicitly modeled faults using elastic-rebound-motivated renewal models. Where the data of last event is unknown, constraints on the open interval could be utilized (the time over which we are certain no event occurred). We might endeavor to apply this nationwide, although results will only differ from Poisson where the open interval is approaching the average recurrence interval on each fault.

Launch new deformation modeling effort

Fault slip rates, specified by deformation models, are among the most critical model constraints when it comes to earthquake hazard and risk, yet they generally remain poorly quantified. This initiative would establish the next-generation deformation models in as many areas as possible, with emphasis on improving slip-rate uncertainties (covariance), off-fault deformation estimates, viscoelastic corrections, and block-rotation effects.

Improve Central and Eastern U.S. (CEUS) fault sources

As discussed by Field et al. (2023) and Jordan et al. (2023), existing USGS CEUS fault-based sources generally assume that only a single-sized event ever occurs on each fault (we just do not yet know what that characteristic magnitude is). This approximation no longer represents best available science and is inconsistent with fault-model applications in other regions. Epistemic uncertainties should also to be redefined (e.g., to achieve the next goal below) and ideally made consistent with those defined in other regions.

Full, nationwide epistemic uncertainty quantification for 2023 NSHM

We have yet to quantify, nationwide, the hazard uncertainties associated with the logic trees defined for the 2023 USGS NSHM (only those for a small set of locations have been examined, and in an approximate manner; e.g., Figure 17 of Petersen et al., 2023). This will presumably require high-performance computing and novel algorithms with respect to sampling all branches.

Inversion-based fault system solutions

These models represent our best representation of large, fault-based ruptures, especially with sampling epistemic uncertainties. In addition to the subduction zones mentioned for the U.S. territories above, the following would presumably benefit from inversion-based fault system solutions: Alaska faults and subduction zone; the Cascadia subduction zone; and the fault system in the New Madrid, MO area. One opportunity, and challenge, is incorporation of liquefaction and

lacustrine paleoseismology constraints. This initiative also involves providing command-line tools that enabling others to re-generate models with customized attributes (e.g., alternative slip rates).

Operationalize statistical seismology processing

Seismicity processing that current and future ERFs depend upon (regional rate and *b-value* estimates, declustering, and seismicity smoothing) could be operationalized by porting to a modern, object-oriented code base (thereby avoiding delays associated with scientists re-running their personal codes every time a minor catalog correction is made). This would also reduce latency in updating induced seismicity hazard estimates, improve reproducibility, and facilitate quantification of historical-seismicity related sampling errors (using simulations from fully time-dependent models). This would also free our statistical seismologists to focus more on scientific advancements.

Enable benchmark risk-metric calculations

This is to begin satisfying the valuation need discuss throughout this document (and under ***Risk related valuation metrics*** *in the previous section*) by initiating benchmark portfolio risk calculations (e.g., average annual dollar loss and loss exceedance curves for canonical portfolios and vulnerability functions). This would involve working with user communities to establish appropriate, public-domain elements for these benchmark calculations.

Coordinate multi-cycle physics-based simulator developments

Consider establishing a working group of current and potential simulator model developers, articulate the various inferences that have and could aid ERF development, strategize resources sharing, establish standardized file formats and evaluation metrics, ensure reproducibility and access to results, and develop a support and maintenance business model. This would presumably be a very long-term endeavor, but results could also impact ongoing ERF development as well.

Develop nationwide, fully time dependent ERFs (including spatiotemporal clustering)

Building off long-term ERFs and recent operational aftershock forecasting developments, we might want to develop at least a prototype model, or set of models with various tradeoffs between efficiency and sophistication (e.g., 2D versus 3D and with-faults versus no-faults).

Model Testing Efforts

We could coordinate with the Collaboratory for the Study of Earthquake Predictability (CSEP; see **Data and Resources**), operationalize standard Turing test comparisons (Page and van Der Elst, 2018), and evaluate model consistency against fragile geologic features.

The above do not represent a complete list of ongoing activities or worthy pursuits. A more detailed compilation of possible improvements can be found in the ERF section of the USGS Earthquake Hazards Program annual external grants announcement (see **Data and Resources** section). The bottom line is there are many interesting and potentially impactful ways we can improve the ERFs used in hazard and risk assessments, including the USGS NSHMs.

Data and Resources

The USGS Earthquake Hazards Program external grants announcement is available at https://www.usgs.gov/programs/earthquake-hazards/science/external-grants-overview (last accessed in Aug., 2024).

The 2017 report from the National Earthquake Prediction Evaluation Council (NEPEC) to the USGS Earthquake Hazards Program referenced in the paper is available at: https://d9-wret.s3.us-west-2.amazonaws.com/assets/palladium/production/s3fs-public/atoms/files/NEPEC_Report_November2017.pdf (last accessed Dec. 2024).

The web site for the Collaboratory for the Study of Earthquake Predictability (CSEP) is: http://cseptesting.org (last accessed Feb., 2025).

Declaration of Competing Interests

The authors declare no competing interests.

Acknowledgements

We thank Gavin Hayes, the Senior Science Advisor for Earthquake and Geologic Hazards at the USGS, for a thoughtful and influential evaluation of this document. We also thank Aybige Akinci and an anonymous individual for equally helpful reviews on behalf of BSSA. In addition, we awe a huge debt of gratitude to the following members of the USGS ERF review panel, especially the chair

(Thomas Jordan) who condensed all their extensive comments into a comprehensive report: Norm Abrahamson, John Anderson, Glenn Biasi , Kenneth Campbell, Timothy Dawson , Matt Gerstenberger, Susan Hough, Thomas Jordan (chair), Yajie Lee, Warner Marzocchi, Badie Rowshandel, Katherine Scharer, David Schwartz , Gabriel Toro, Ray Weldon, and Ivan Wong. We also acknowledge the skill and patience of Amber Hess with respect to developing Figure 2, plus the extensive editorial comments from Brian Shiro and Kristen Marra in obtaining USGS publication approval. PMM and OZ were supported by King Abdullah University of Science and Technology (KAUST), grant BAS/1/1339-01-01. Any use of 1618 trade, firm, or product names is for descriptive purposes only and does not imply endorsement by the U.S. Government.

References

Aalsburg, J., J. Rundle, L. Grant Ludwig, P. Rundle, G. Yakovlev, D. Turcotte, A. Donnellan, K. Tiampo, and J. Fernandez (2010). Space- and Time-Dependent Probabilities for Earthquake Fault Systems from Numerical Simulations: Feasibility Study and First Results, *Pure and Applied Geophys.* **167**, 967-977, doi: 10.1007/s00024-010-0091-3.

Abrahamson, N. A., N. M. Kuehn, M. Walling, and N. Landwehr (2019). Probabilistic Seismic Hazard Analysis in California Using Nonergodic Ground-Motion Models, *Bull. Seismol. Soc. Am.* **109**, 1235–1249, doi: 10.1785/0120190030.

American Society of Civil Engineers (2023). Seismic Evaluation and Retrofit of Existing Buildings, doi: 10.1061/9780784416112.

Anderson, J. G., and J. N. Brune (1999). Probabilistic Seismic Hazard Analysis without the Ergodic Assumption. *Seismol. Res. Lett.* **70**, 19–28, doi: 10.1785/gssrl.70.1.19

Anderson, J. G., G. P. Biasi, S. Angster, and S. G. Wesnousky (2021). Improved scaling relationships for seismic moment and average slip of strike-slip earthquakes incorporating fault-slip rate, fault width, and stress drop, *Bull. Seismol. Soc. Am.* **111**, 2379–2392, doi: 10.1785/0120210113

Andrews, D. J., and E. Schwerer (2000). Probability of rupture of multiple fault segments, *Bull. Seismol. Soc. Am.* **90**, 1498–1506, doi: 10.1785/0119990163

Balay, S., S. Abhyankar, M. F. Adams, S. Benson, J. Brown, P. Brune, K. Buschelman, E. M. Constantinescu, L. Dalcin, A. Dener, V. Eijkhout, J. Faibussowitsch, W. D. Gropp, V. Hapla, T. Isaac, P. Jolivet, D. Karpeev, D. Kaushik, M. G. Knepley, F. Kong, S. Kruger, D. A. May, L. McInnes, Curfman, R. Mills, Tran, L. Mitchell, T. Munson, R. E. Roman, K. Rupp, P. Sanan, J. Sarich, B. F. Smith, S. Zampini, H. Zhang, and J. Zhang (2023). PETSc/TAO Users Manual (Rev. 3.20), 303 pp., doi: 10.2172/2205494.

Bazzurro, P., C. Cornell, C. Menun, M. Motahari, and N. Luco (2006). Advanced Seismic Assessment Guidelines, *PEER Report 2006-05. Pacific Earthquake Engineering Research Center*, University of California, Berkeley, CA. https://peer.berkeley.edu/publications/2006-05

Ben-Zion, Y. (2008). Collective behavior of earthquakes and faults: Continuum discrete transitions, evolutionary changes and corresponding dynamic regimes, *Rev. Geophys.* **46**, RG4006, doi: 10.1029/2008RG000260.

Ben-Zion, Y., K. Dahmen, V. Lyakhovsky, D. Ertas, and A. Agnon (1999). Self-driven mode switching of earthquake activity on a fault system, *Earth Planet. Sci. Lett.* **172**, 11–21, doi: 10.1016/S0012-821X(99)00187-9.

Biasi, G. P., and S. G. Wesnousky (2016). Steps and gaps in ground ruptures: Empirical bounds on rupture propagation, *Bull. Seismol. Soc. Am.* **106**, 1110–1124, doi: 10.1785/0120150175.

Biasi, G. P., and S. G. Wesnousky (2017). Bends and ends of surface ruptures, *Bull. Seismol. Soc. Am.* **107**, 2543–2560, doi: 10.1785/0120160292.

Biasi, G. P. and K. M. Scharer (2019). The Current Unlikely Earthquake Hiatus at California's Transform Boundary Paleoseismic Sites. *Seismol. Res. Lett.* **90**, 1168–1176. doi: 10.1785/0220180244

Biemiller, J., A.-A. Gabriel, D.A. May, and L. Staisch (2024), Subduction zone geometry modulates the megathrust earthquake cycle: magnitude, recurrence, and variability, *J. Geophys. Res. – Solid Earth,* **129**, e2024JB029191, doi: 10.1029/2024JB029191..

Blowes, K., P Kourehpaz, and C. Molina Hutt (2023). Risk-targeted seismic evaluation of functional recovery performance in buildings, *Earthquake Engineering & Structural Dynamics*, **52, 4245-4264**, doi: 10.1002/eqe.3984.

Box, G. E. P. (1980). Sampling and Bayes inference in scientific modelling and robustness, *J. Roy Stat. Soc. Ser. A* **143**, 383–430, doi: 10.2307/2982063..

Building Seismic Safety Council (BSSC) (2020). *NEHRP recommended seismic provisions for new buildings and other structures*, Federal Emergency Management Agency (FEMA) report no. P-2082-1, 555 pp.. Available at: https://www.fema.gov/sites/default/files/2020-10/fema_2020-nehrp-provisions_part-1-and-part-2.pdf (accessed 22 November 2023)

Cattania, C., M. J. Werner, W. Marzocchi, S. Hainzl, D. Rhoades, M. Gerstenberger, M. Liukis, W. Savran, A. Christophersen, A. Helmstetter, A. Jimenez, S. Steacy, and T. H. Jordan (2018). The Forecasting Skill of Physics-Based Seismicity Models during the 2010–2012 Canterbury, New Zealand, Earthquake Sequence. *Seismol. Res. Lett.* **89**, 1238–1250, doi: 10.1785/0220180033

Cochran, E. S., J. L. Rubinstein, A. J. Barbour, and J. O. Kaven (2024). Induced seismicity strategic vision, *U.S. Geological Survey Circular 1509*, 39 pp., doi: 10.3133/cir1509.

Coppersmith, K. J., L. A. Salomone, C. W. Fuller, L. L. Glaser, K. L. Hanson, R. D. Hartleb, W. R. Lettis, S. C. Lindvall, S. M. McDuffie, R. K. McGuire, et al. (2012). Central and Eastern United States seismic source characterization for nuclear facilities, *U.S. Nuclear Regulatory Commission (NRC) Rept. NUREG-2115, U.S. Department of Energy (DOE) Rept. DOE/NE-0140, and Electric Power Research Institute (EPRI) Rept. 1021097*, 3176 pp., doi: 10.2172/1041187.

Cua, G. and T. Heaton (2007). The Virtual Seismologist (VS) Method: a Bayesian Approach to Earthquake Early Warning. In: Gasparini, P., Manfredi, G., Zschau, J. (eds) Earthquake Early Warning Systems (pp. 97-132). Springer, Berlin, Heidelberg. doi: 10.1007/978-3-540-72241-0_7.

Dahmen, K., D. Ertas, and Y. Ben-Zion (1998). Gutenberg–Richter and characteristic earthquake behavior in simple mean-field models of heterogeneous faults, *Phys. Rev. E* **58**, 1494–1501, doi: 10.1103/PhysRevE.58.1494.

1603 Danciu, L., D. Giardini, G. Weatherill, R. Basili, R. Nandan, A. Rovida, C. Beauval, P.-Y. Bard, M. Pagani,
1604 C. G. Reyes, K. Sesetyan, S. Vilanova, F. Cotton, and S. Wiemer (2024). The 2020 European
1605 Seismic Hazard Model:)verview and results, *Nat. Hazards Earth Syst. Sci.* **24**, 3049–3073, doi:
1606 10.5194/nhess-24-3049-2024.

1607

1608 Dascher-Cousineau, K., O. Shchur, E. Brodsky, and S. Günnemann (2023). Using deep learning for
1609 flexible and scalable earthquake forecasting, *Geophys. Res. Lett.* **50**, e2023GL103909, doi:
1610 10.1029/2023GL103909

1611

1612 Dieterich, H. H. (1994). A constitutive law for rate of earthquake production and its application to
1613 earthquake clustering, *J. Geophys. Res.,* **99**, 2601–2618, doi: 10.1029/93JB02581.

1614

1615 Dieterich, J. H., and K. B. Richards-Dinger (2010). Earthquake recurrence in simulated fault systems,
1616 *Pure Appl. Geophys.* **167**, 1087–1184 , doi: 10.1007/ s00024-010-0094-0.

1617

1618 Dolan, J. F., D. D. Bowman, and C. G. Sammis (2007). Long-range and long-term fault interactions in
1619 southern California, *Geology* **35**, 855–858, doi: 10.1130/G23789A.1.

1620

1621 Electric Power Research Institute/Department of Energy/Nuclear Regulatory Commission
1622 (EPRI/DOE/NRC) (2012). Central and eastern United States seismic source characterization for
1623 nuclear facilities, *NUREG-2115*, EPRI, USDOE, and USNRC, Palo Alto, California.

1624

1625 Ellsworth, W. L. (2013). Injection-induced earthquakes, *Science*, **341**, doi:
1626 10.1126/science.1225942.

1627

1628 Erickson, B. A., J. Jiang, V. Lambert, S. D. Barbot, M. Abdelmeguid, M. Almquist, J.-P. Ampuero, R.
1629 Ando, C. Cattania, A. Chen, L. D. Zilio, S. Deng, E. M. Dunham, A. E. Elbanna, A.-A. Gabriel, T. W.
1630 Harvey, Y. Huang, Y. Kaneko, J. E. Kozdon, N. Lapusta, D. Li, M. Li, C. Liang, Y. Liu, S. Ozawa, A.
1631 Perez-Silva, C. Pranger, P. Segall, Y. Sun, P. Thakur, C. Uphoff, Y. van Dinther, and Y. Yang (2023).
1632 Incorporating Full Elastodynamic Effects and Dipping Fault Geometries in Community Code
1633 Verification Exercises for Simulations of Earthquake Sequences and Aseismic Slip (SEAS), *Bull.*
1634 *Seismol. Soc. Am.* **113**, 499–523. doi: 10.1785/0120220066

1635

1636 Field, E. H., T. H. Jordan, and C. A. Cornell (2003). OpenSHA: A developing community-modeling
1637 environment for seismic hazard analysis, *Seismol. Res. Lett.* **74**, 406–419, doi:
1638 10.1785/gssrl.74.4.406.

Field, E. H., and M. T. Page (2011). Estimating earthquake-rupture rates on a fault or fault system, *Bull. Seismol. Soc. Am.* **101**, 79–92, doi: 10.1785/0120100004.

Field, E. H., R. J. Arrowsmith, G. P. Biasi, P. Bird, T. E. Dawson, K. R. Felzer, D. D. Jackson, K. M. Johnson, T. H. Jordan, C. Madden, A. J. Michael, K. R. Milner, M. T. Page, T. Parsons, P. M. Powers, B. E. Shaw, W. R. Thatcher, R. J. Weldon, and Y. Zeng (2014). Uniform California Earthquake Rupture Forecast, version 3 (UCERF3)—The time-independent model, *Bull. Seism. Soc. Am.* **104**, 1122–1180, doi: 10.1785/0120130164.

Field, E. H., R. J. Arrowsmith, G. P. Biasi, P. Bird, T. E. Dawson, K. R. Felzer, D. D. Jackson, K. M. Johnson, T. H. Jordan, C. Madden, et al. (2015). Long-term, time-dependent probabilities for the Third Uniform California Earthquake Rupture Forecast (UCERF3), *Bull. Seismol. Soc. Am.* **105**, 511–543, doi: 10.1785/0120140093.

Field, E. H., T. H. Jordan, L. M. Jones, A. J. Michael, M. L. Blanpied, and Other Workshop Participants (2016). The Potential Uses of Operational Earthquake Forecasting. *Seismol. Res. Lett.* **87**, 313–322. doi: 10.1785/0220150174

Field, E. H., T. H. Jordan, M. T. Page, K. R. Milner, B. E. Shaw, T. E. Dawson, G. P. Biasi, T. Parsons, J. L. Hardebeck, A. J. Michael, R. J. Weldon II, P. M. Powers, K. M. Johnson, Y. Zeng, P. Bird, K. R. Felzer, N. van der Elst, C. Madden, R. Arrowsmith, M. J. Werner, W. R. Thatcher, and D. D. Jackson (2017). A Synoptic View of the Third Uniform California Earthquake Rupture Forecast (UCERF3), *Seismol. Res. Lett.* **88**, 1259–1267, doi: 10.1785/0220170045.

Field, E. H., K. Porter, and K. Milner (2017). A prototype operational earthquake loss model for California based on UCERF3-ETAS—A first look at valuation, *Earthq. Spectra* **33**, no. 4, 1279–1299, doi: 10.1193/011817EQS017M.

Field, E. H. and K. R. Milner (2018). Candidate Products for Operational Earthquake Forecasting Illustrated Using the HayWired Planning Scenario, Including One Very Quick (and Not-So-Dirty) Hazard-Map Option. *Seismol. Res. Lett.* **89**, 1420–1434. doi: 10.1785/0220170241

Field, E. H., K. R. Milner, and M. T. Page (2020). Generalizing the inversion-based PSHA source model for an interconnected fault system, *Bull. Seismol. Soc. Am.* **111**, 371–390, doi: 10.1785/0120200219.

Field, E. H., K. R. Milner, M. T. Page, W. H. Savran, and N. van der Elst (2021). Improvements to the Third Uniform California Earthquake Rupture Forecast ETAS Model (UCERF3-ETAS), *The Seismic Record* **1**, 117–125, doi: 10.1785/0320210017.

Field, E. H., K. R. Milner, A. E. Hatem, P. M. Powers, F. F. Pollitz, A. L. Llenos, Y. Zeng, K.M. Johnson, B. E. Shaw, D. McPhillips, et al. (2023). The USGS 2023 conterminous U.S. time-independent earthquake rupture forecast, *Bull. Seismol. Soc. Am.* **114**, 523-571, https://doi.org/10.1785/0120230120.

Frankel, A. (1995). Mapping seismic hazard in the central and eastern United States, *Seismol. Res. Lett.* **66**, 8-21, doi: 10.1785/gssrl.66.4.8.

Gardner, J. K., and L. Knopoff (1974). Is the sequence of earthquakes in southern California with aftershocks removed Poissonian?, *Bull. Seismol. Soc. Am.* **64**, 1363–1367, doi: 10.1785/BSSA0640051363.

Gerstenberger, M. C., S. Wiemer, and L. Jones (2004). Real-time forecasts of tomorrow's earthquakes in California: A new mapping tool, *USGS Open-File Report 2004-1390*, doi: 10.3133/ofr20041390.

Gerstenberger, M. C., G. McVerry, D. Rhoades, and M. Stirling (2014). Seismic hazard modeling for the recovery of Christchurch. *Earthquake Spectra* **30**, 17-29, doi: 10.1193/021913EQS037M.

Gerstenberger, M. W. Marzocchi, T. Allen, M. Pagani, J. Adams, L. Danciu, E. Field, H. Fujiwara, N. Luco, K.-F. Ma, C. Meletti, and M. Petersen (2020). Probabilistic Seismic Hazard Analysis at Regional and National Scales: State of the Art and Future Challenges. *Reviews of Geophysics*, **58**, e2019RG000653, doi: . 10.1029/2019RG000653.

Gerstenberger, M.C., R. Van Dissen, C. Rollins, C. DiCaprio, K. K.Thingbaijim, S. Bora, C. Chamberlain, A. Christophersen, G. L.Coffey, S. M. Ellis, and P. Iturrieta (2024). The seismicity rate model for the 2022 Aotearoa New Zealand national seismic hazard model. *Bull. Seismol. Soc. Am.* **114,** 182-216, doi: 10.1785/0120230165.

Gerstenberger, M. C., S. Bora, B. A. Bradley, C. DiCaprio, A. Kaiser, E. F. Manea, A. Nicol, C. Rollins, M. W. Stirling, K. K. S. Thingbaijam, et al. (2023). The 2022 Aotearoa New Zealand National Seismic

1710 Hazard Model: Process, Overview, and Results, *Bull, Seismol. Soc. of Am.* **114**,7–36,
1711 doi: 10.1785/0120230182

1712

1713 Goda, K., W. Friedemann, and D. James. (2014). Insurance and Reinsurance Models for Earthquake,
1714 In: Beer, M., Kougioumtzoglou, I., Patelli, E., Au, IK. (eds) *Encyclopedia of Earthquake*
1715 *Engineering* 1830 (pp. 1–29). Springer, Berlin, Heidelberg, doi: 10.1007/978-3-642-36197-5.

1716

1717 Goldfinger, C., Y. Ikeda, R. S. Yeats, and J. Ren (2013). Superquakes and supercycles, *Seismol. Res. Lett.*
1718 **84**, 24-32, doi: 10.1785/0220110135.

1719

1720 Grant, L. B., and K. Sieh (1994). Paleoseismic evidence of clustered earthquakes on the San Andreas
1721 fault in Carrizo Plain, California, *J. Geophys. Res.* **99**, 6819–6841, doi: 1837 10.1029/94JB00125.

1722

1723 Guns, K. A., R. A. Bennett, J. C. Spinler, and S. F. McGill (2021). New geodetic constraints on southern
1724 San Andreas fault-slip rates, San Gorgonio Pass, California: *Geosphere*, **17**, 39– 68, doi:
1725 10.1130/GES02239.1.

1726

1727 Hardebeck, J. L. (2021). Spatial clustering of aftershocks impacts the performance of physics-based
1728 earthquake forecasting models, *J. Geophys. Res. Solid Earth* **126**, e2020JB020824, doi:
1729 10.1029/2020JB020824 .

1730

1731 Hardebeck, J. L. and R. A. Harris (2022). Earthquakes in the Shadows: Why Aftershocks Occur at
1732 Surprising Locations. *The Seismic Record* **2**, 207–216, doi: 10.1785/0320220023.

1733

1734 Harris, R. A., M. Barall, R. Archuleta, E. Dunham, B. Aagaard, J. P. Ampuero, H. Bhat, V. Cruz-Atienza, L.
1735 Dalguer, P. Dawson, et al. (2009). The SCEC/USGS dynamic earthquake rupture code veri- fication
1736 exercise, *Seismol. Res. Lett.* **80**, 119–126, doi: 10.1785/gssrl.80.1.119.

1737

1738 Harris, R. A., M. Barall, B. Aagaard, S. Ma, D. Roten, K. Olsen, B. Duan, D. Liu, B. Luo, K. Bai, J.-P.
1739 Ampuero, Y. Kaneko, A.-A. Gabriel, K. Duru, T. Ulrich, S. Wollherr, Z. Shi, E. Dunham, S. Bydlon, Z.
1740 Zhang, X.Chen, S. N. Somala, C. Pelties, J. Tago, V. M. Cruz-Atienza, J. Kozdon, E. Daub, K. Aslam, Y.
1741 Kase, K. Withers, NS L. Dalguer (2018). A Suite of Exercises for Verifying Dynamic Earthquake
1742 Rupture Codes. *Seismol. Res. Lett.* **89**, 1146–1162, doi: 10.1785/0220170222.

1743

Hatem, A. E. and J. F. Dolan (2018). A Model for the Initiation, Evolution, and Controls on Seismic Behavior of the Garlock Fault, California, *Geochemistry, Geophysics, Geosystems* **19**, 2166-2178, doi: 10.1029/2017GC007349.

Hatem, A. E., N. Reitman, R. Briggs, R. Gold, and J. Thompson Jobe (2022). Western U.S. geologic deformation model for use in the U.S. National Seismic Hazard Model 2023, *Seismol. Res. Lett.* **93**, 3053–3067, doi: 10.1785/0220220154.

Hayes, G., A. S. Baltay Sundstrom, W. D. Barnhart, M. L. Blanpied, L. A. Davis, P. S. Earle, N. Field, J. M. Franks, D. D. Given, R. D. Gold, C. A. Goulet, M. M. Guy, J. L. Hardebeck, N. Luco, F. Pollitz, A. T. Ringler, K. M. Scharer, S. Sobieszczyk, V. I. Thomas, and C. J. Wolfe et al. (2024). USGS Earthquake Hazards Program Decadal Science Strategy, 2024-33, *U.S. Geological Survey Circular 1544*, 55 pp., doi: 10.3133/cir1544.

Hecker, S., N. A. Abrahamson, and K. E. Wooddell (2013). Variability of displacement at a point: Implications for earthquake-size distribution and rupture hazard on faults, *Bull. Seismol. Soc. Am.* **103**, 651–674, doi: 10.1785/0120120159.

Hearn, E. H. (2022). "Ghost transient" corrections to the southern California GPS velocity field from San Andreas fault seismic cycle models, *Seismol. Res. Lett.* **93**, 2793–2989, doi: 10.1785/0220220156.

Helmstetter, A., Y. Y. Kagan, and D. D. Jackson (2007). High-resolution time-independent grid-based forecast for M >=5 earthquakes in California, *Seismol. Res. Lett.* **78**, 78–86, doi: 10.1785/gssrl.78.1.78.

Iturrieta, P., M. C. Gerstenberger, C. Rollins, R. Van Dissen, Ti. Wang, and D. Schorlemmer (2024). Accounting for the Variability of Earthquake Rates within Low-Seismicity Regions: Application to the 2022 Aotearoa New Zealand National Seismic Hazard Model. *Bull. Seismol. Soc. Am.* **114**, 217–243, doi: 10.1785/0120230164

Jaiswal K. S., J. Rozelle, M. Tong, A. Sheehan, S. McNabb, M. Kelly, C. Zuzak, D. Bausch, and J. Simms (2023). Hazus estimated annualized earthquake losses for the United States. *Federal Emergency Management (FEMA) report no. P-366, 96 pp.*. https://www.fema.gov/sites/default/files/documents/fema_p-366-hazus-estimated-annualized-earthquake-losses-united-states.pdf (accessed May 24, 2025).

Jiang J., B. A. Erickson, V. R. Lambert, J.-P. Ampuero, R. Ando, S. D. Barbot, C. Cattania, L. D. Zilio, B. Duan, E. M. Dunham, A.-A. Gabriel, N. Lapusta, D. Li, M. Li, D. Liu, Y. Liu, S. Ozawa, C. Pranger, and Y. van Dinther (2022). Community-Driven Code Comparisons for Three-Dimensional Dynamic Modeling of Sequences of Earthquakes and Aseismic Slip, *J. Geophys. Res. Solid Earth* **127**, e2021JB023519, doi: 10.1029/2021JB023519

Johnson, K. J., J. R. Murray, and C. Wespestad (2022). Creep rate models for the 2023 US National Seismic Hazard Model: Physically constrained inversions for the distribution of creep on California faults, *Seismol. Res. Lett.* **93**, 3151–3169, doi: 10.1785/0220220186.

Johnson, K. J., W. C. Hammond, and R. Weldon (2024). Review of geodetic and geologic deformation models of 2023 US National Seismic Hazard Model, *Bull. Seismol. Soc. Am.* ***114****, 1407-1436,* doi: 10.1785/0120230137*.*

Jordan, T. H., and L. M. Jones (2010). Operational earthquake forecasting: Some thoughts on why and how, *Seismol. Res. Lett.* **81**, 571–574, doi: 10.1785/gssrl.81.4.571.

Jordan, T. H., W. Marzocchi, A. J. Michael, and M. C. Gerstenberger (2014). Operational earthquake forecasting can enhance earthquake preparedness, *Seismol. Res. Lett.* **85**, 955–959, doi: 10.1785/0220140143.

Jordan, T. H., N. Abrahamson, J. G. Anderson, G. Biasi, K. Campbell, T. Dawson, H. DeShon, M. Gerstenberger, N. Gregor, K. Kelson, et al. (2023). Panel review of the USGS 2023 conterminous U.S. time-independent earthquake rupture forecast, *Bull. Seismol. Soc. Am.* **114**, 572-607, doi: 10.1785/0120230140.

King, G. C. P., R. S. Stein, and J. Lin (1994). Static stress changes and the triggering of earthquakes, *Bull. Seism. Soc. Am.* **84**, 935-953, doi: 10.1785/BSSA0840030935.

King. G. C. P. and S. G. Wesnousky (2007). Scaling of fault parameters for continental strike-slip earthquakes, *Bull. Seismol. Soc. Am.* **97**, 1833-1840, doi: 10.1785/0120070048.

Llenos, A. L. and A. J. Michael (2013) Modeling earthquake rate changes in Oklahoma and Arkansas—Possible signatures of induced seismicity: *Bull. Seismol. Soc. Am.* **103**, 2850–2861, doi: 10.1785/0120130017

1817 Llenos, A. L. and N. J. van der Elst (2019). Improving Earthquake Forecasts during Swarms with a
1818 Duration Model, *Bull. Seismol. Soc. Am.* **109**, 1148–1155, doi: 10.1785/0120180332.

1819

1820 Llenos, A. L. and A. J. Michael (2019). Ensembles of ETAS Models Provide Optimal Operational
1821 Earthquake Forecasting During Swarms: Insights from the 2015 San Ramon, California
1822 Swarm, *Bull. Seismol. Soc. Am.* **109**, 2145–2158, doi: 10.1785/0120190020.

1823

1824 Llenos, A. L., and A. J. Michael (2020). Regionally Optimized Background Earthquake Rates from
1825 ETAS (ROBERE) for probabilistic seismic hazard assessment, *Bull. Seismol. Soc. Am.* **110**,
1826 1172–1190, doi: 10.1785/0120190279.

1827

1828 Llenos, A. L., A. J. Michael, A. M. Shumway, J. L. Rubinstein, K. L. Haynie, M. P. Moschetti, J. M.
1829 Altekruse, and K. R. Milner (2024). Forecasting the Long-Term Spatial Distribution of
1830 Earthquakes for the 2023 U.S. National Seismic Hazard Model Using Gridded Seismicity,
1831 *Bull. Seismol. Soc. Am.* **110**, 1736–1751, doi: 10.1785/0120230220

1832

1833 Mancini, S., M. Segou, M. Werner, and T. Parsons (2020), The predictive skills of elastic coulomb
1834 rate-and-state aftershock forecasts during the 2019 Ridgecrest, California, earthquake
1835 sequence, *Bull. Seismol. Soc. Am.* **110**, 1736-1751, doi: 10.1785/0120200028.

1836

1837 Marzocchi, W. and T. H. Jordan (2018). Experimental concepts for testing probabilistic earthquake
1838 forecasting and seismic hazard models, *Geophys. J. Int.* **215**, 780–798, 10.1093/gji/ggy276.

1839

1840 Mayeda, K., A. Hofstetter, J. L. O'Boyle, and W. R. Walter (2003). Stable and transportable regional
1841 magnitudes based on coda-derived moment-rate spectra. *Bull. Seismol. Soc. Am.* ***93***, 224-239,
1842 doi: 10.1785/0120020020.

1843

1844 McPhillips, D. (2022). Revised earthquake recurrence intervals in California, U.S.A.: New
1845 paleoseismic sites and application of event likelihoods, *Seismol. Res. Lett.* **93**, 3009–3023, doi:
1846 10.1785/0220220127.

1847

1848 Meletti, C., W. Marzocchi, V. D'Amico, G. Lanzano, L. Luzi, F. Martenelli, B. Pace, A. Rovida, M. Taroni,
1849 and F. Vasini (2021). The New Italian Seismic Hazard Model (MPS19), *Annals of Geophysics*, **64**,
1850 SE112, doi: 10.4401/ag-8579

1851

1852 Mizrahi, L., I. Dallo, N. J. van der Elst, A. Christophersen, I. Spassiani, M. J. Werner, et al.
1853 (2024). Developing, testing, and communicating earthquake forecasts: Current practices and
1854 future directions. *Reviews of Geophysics* **62**, e2023RG000823, doi: 10.1029/2023RG000823.

1855

1856 Michael, A. J. and M. J. Werner (2018). Preface to the Focus Section on the Collaboratory for the
1857 Study of Earthquake Predictability (CSEP): New Results and Future Directions. *Seismol. Res.*
1858 *Lett.* **89**, 1226–1228, doi: 10.1785/0220180161

1859

1860 Michael, A. J., S. K. McBride, J. L. Hardebeck, M. Barall, E. Martinez, M. T. Page, N. van der Elst, E. H.
1861 Field, K. R. Milner, and A. M. Wein (2019). Statistical Seismology and Communication of the
1862 USGS Operational Aftershock Forecasts for the 30 November 2018 Mw 7.1 Anchorage, Alaska,
1863 Earthquake, *Seismol. Res. Lett.*, **91**, 153–173, doi: 10.1785/0220190196.

1864

1865 Milner, K. R., E. H. Field, W. H. Savran, M. T. Page, and T. H. Jordan (2020). Operational earthquake
1866 forecasting during the 2019 Ridgecrest, California, earthquake sequence with the UCERF3- ETAS
1867 model, *Seismol. Res. Lett.* **91**, 1567–1578, doi: 10.1785/0220190294.

1868

1869 Milner, K. R., B. E. Shaw, C. A. Goulet, K. B. Richards-Dinger, S. Callaghan, T. H. Jordan, J. H. Dieterich,
1870 and E. H. Field (2021). Toward physics-based nonergodic PSHA: A prototype fully deterministic
1871 seismic hazard model for southern California, *Bull. Seismol. Soc. Am.* **111**, 898–915, doi:
1872 10.1785/0120200216.

1873

1874 Milner, K. R., B. E. Shaw, and E. H. Field (2022). Enumerating plausible multifault ruptures in
1875 complex fault systems with physical constraints, *Bull. Seismol. Soc. Am.* **112**, 1806–1824, doi:
1876 10.1785/0120210322.

1877

1878 Milner, K. R., and E. H. Field (2023). A comprehensive fault system inversion approach: Methods
1879 and application to NSHM23, *Bull. Seismol. Soc. Am.* **114**, 486-522, doi: 10.1785/0120230122.

1880

1881 Mohammadi, J. and A. Heydari (2008). Seismic and Wind Load Considerations for Temporary
1882 Structures, *Practice Periodical on Structural Design and Construction* **13**, 128-134, doi:
1883 10.1061/(ASCE)1084-0680(2008)13:3(128).

1884

1885 Mueller, C. S. (2019). Earthquake catalogs for the USGS National Seismic Hazard Maps, *Seismol. Res.*
1886 *Lett.* **90**, 251–261, doi: 10.1785/0220170108.

1887

National Institute of Standards and Technology - Federal Emergency Management Agency (NIST-FEMA) (2021). Recommended Options for Improving the Built Environment for Post-Earthquake Reoccupancy and Functional Recovery Time, *FEMA Special Publication FEMA P-2090/NIST SP-1254*, 115 pp., doi: 10.6028/NIST.SP.1254

Norbeck, J. H. and J. L. Rubinstein (2018). Hydromechanical earthquake nucleation model forecasts onset, peak, and falling rates of induced seismicity in Oklahoma and Kansas: *Geophys. Res. Lett.* **45**, 2963–2975, doi: 10.1002/2017GL076562.

Ogata, Y. (1988). Statistical models of point occurrences and residual analysis for point processes, *J. Am. Stat. Assoc.* **83**, 9–27, doi: 10.2307/2288914.

Ogata, Y. (1998). Space-time point-process models for earthquake occurrences, *Ann. Inst. Statist. Math.*, **50**, 379–402, doi: 10.1023/A:1003403601725.

Pacific Earthquake Engineering Research Center (2017). Guidelines for Performance-Based Seismic Design of Tall Buildings, *Pacific Earthquake Engineering Research Center (PEER) Report 2017/06*, University of California, Berkeley, 147 pp., https://peer.berkeley.edu/sites/default/files/final_tbi_report_10.9.2017_0.pdf (accessed Feb 24, 2025).

Page, M. T., E. H. Field, K. R. Milner, and P. M. Powers (2014). The UCERF3 grand inversion: Solving for the long-term rate of ruptures in a fault system, *Bull. Seismol. Soc. Am.* **104**, 1181–1204, doi: 10.1785/0120130180.

Page, M. T., N. van der Elst, J. Hardebeck, K. Felzer, and A. J. Michael; Three Ingredients for Improved Global Aftershock Forecasts: Tectonic Region, Time-Dependent Catalog Incompleteness, and Intersequence Variability (2016). *Bull. Seismol. Soc. Am.* **106**, 2290–2301. doi: 10.1785/0120160073

Page, M. T and N. J. van der Elst (2018). Turing-Style Tests for UCERF3 Synthetic Catalogs. *Bull. Seismol. Soc. Am.* **108**, 729–741. doi: 10.1785/0120170223

Parsons, T. and D. S. Dreger, (2000). Static-stress impact of the 1992 Landers earthquake sequence on nucleation and slip at the site of the 1999 M= 7.1 Hector Mine earthquake, southern California, *Geophys. Res. Lett.* **27** 1949–1952, doi: 10.1029/1999GL011272.

Parsons, T. (2002), Global Omori law decay of triggered earthquakes: Large aftershocks outside the classical aftershock zone, *J. Geophys. Res.* **107**, 2199, doi: 10.1029/2001JB000646.

Parsons, T., C. Ji, and E. Kirby (2023), Evaluating a prospective fault-based stress-transfer forecast for the M7.9 Wenchuan earthquake region, 15 years later, *The Seismic Record* **3**, 218-227, doi:10.1785/0320230021.

Petersen, M. D., C. S. Mueller, M. P. Moschetti, S. M. Hoover, A. L. Llenos, W. L. Ellsworth, A. J. Michael, J. L. Rubinstein, A. F. McGarr, and K. S. Rukstales (2016), 2016 one-year seismic hazard forecast for the central and eastern United States from induced and natural earthquakes, *U.S. Geological Survey Open-File Report 2016-1035*, 52 pp., https://doi.org/10.3133/ofr20161035(accessed Feb 24, 2025).

Petersen, M. D., C. S. Mueller, M. P. Moschetti, S. M. Hoover, A. M. Shumway, D. E. McNamara, R. A. Williams, A. L. Llenos, W. L. Ellsworth, A. J. Michael, J. L. Rubinstein, A. F. McGarr, and K.S. Rukstales (2017). 2017 0ne-year seismic-hazard forecast for the central and eastern United States from induced and natural earthquakes: *Seismol. Res. Lett.* **88**, 772–783, doi: 10.1785/0220170005.

Petersen, M.D., C. S. Mueller, M. P. Moschetti, S. M. Hoover, K. S. Rukstales, D. E. McNamara, R. A. Williams, et al. (2018). 2018 one-year seismic hazard forecast for the central and eastern United States from induced and natural earthquakes, *Seismol. Res. Lett.* **89**, 1049–1061, doi: 10.1785/0220180005.

Petersen, M. D., A. M. Shumway, P. M. Powers, M. P. Moschetti, A. L. Llenos, A. J. Michael, C. S. Mueller, A. D. Frankel, S. Rezaiean, K. S. Rukstales, D. E. McNamara, P. G. Okubo, Y. Zeng, K. S. Jaiswal, S. K. Ahdi, J. M. Altekruse, and B. R. Shiro (2021). 2021 US National Seismic Hazard Model for the state of Hawaii, *Earthquake Spectra* **38**, 865–916, doi: 10.1177/87552930211052061.

Petersen, M. D., A. M. Shumway, P. M. Powers, E. H. Field, M. P. Moschetti, K. S. Jaiswal, K. R. Milner, S. Rezaeian, A. D. Frankel, A. L. Llenos, et al. (2023). The 2023 U.S. 50-State National Seismic Hazard Model: Overview and implications, *Earthq. Spectra* **40**, 5-88, doi: 10.1177/87552930231215428.

Pollitz, F. F., E. L. Evans, E. H. Field, A. E. Hatem, E. H. Hearn, K. Johnson, J. R. Murray, P. M. Powers, Z.-K. Shen, C. Wespestad, and Y. Zeng (2022). Western U.S. deformation models for the 2023 update to the U.S. National Seismic Hazard Model, *Seismol. Res. Lett.* **93**, 3068–3086, doi: 10.1785/0220220143.

Powers, P. M., J. M. Altekruse, A. L. Llenos, A. J. Michael K. L. Haynie, P. J. Haeussler, A. M. Bender, S. Rezaeian, M. P. Moschetti, J. A. Smith, R. W. Briggs, R. C. Witter, C. S. Mueller, Y. Zeng, D. L. Girot, J. A. Herrick, A. M. Shumway, and M. D. Petersen (2024). The 2023 Alaska National Seismic Hazard Model, *Earthquake Spectra* **40**, 2545-2597, doi: 10.1177/87552930241266741.

Reasenberg, P. A., and L. M. Jones (1989). Earthquake hazard after a mainshock in California, *Science* **243**, 1173–1176, doi: 10.1126/science.243.4895.1173.

Reasenberg, P. A., and L. M. Jones (1994). Earthquake aftershocks: Update, *Science* **265**, 1251–1252, doi: 10.1126/science.265.5176.1251.

Reid, H. F. (1910). The Elastic-Rebound Theory of Earthquakes. *Bulletin of the Department of Geology, University of California Publications* **6**, 413-444.

Richards-Dinger, K., and J. H. Dieterich (2012). RSQSim earthquake simulator, *Seismol. Res. Lett.* **83**, 983-990, doi: 10.1785/0220120105.

Rockwell, T. K., T. E. Dawson, J. Young, and G. Seitz (2014). A 21 event, 4,000-year history of surface ruptures in the Anza seismic gap, San Jacinto fault: Implications for long-term earthquake production on a major plate boundary fault, *Pure Appl. Geophys.* **172**, 1143-1165, doi: 10.1007/s00024-014-0955-z.

Rodriguez Padilla, A. M., M. E. Oskin, E. E. Brodsky, K. Dascher-Cousineau, V. Herrera, and S. White (2024). The Influence of fault geometrical complexity on surface rupture length. *Geophys. Res. Lett.* **51**, e2024GL109957, doi: 10.1029/2024GL109957.

Roeloffs, E., and J. Goltz (2017). The California Earthquake Advisory Plan: A history, *Seismol. Res. Lett.* **88**, 784–797, doi: 10.1785/0220160183.

Rubinstein, J. L., A. J. Barbour and J. H. Norbeck (2021). Forecasting induced earthquake hazard

using a hydromechanical earthquake nucleation model, *Seismol. Res. Lett.* **92**, 2206–2220, doi: 10.1785/0220200215.

Savran, W. H., M. J. Werner, W. Marzocchi, D. A. Rhoades, D. D. Jackson, K. Milner, E. H. Field, and A. Michael (2020). Pseudoprospective evaluation of UCERF3-ETAS forecasts during the 2019 Ridgecrest sequence, *Bull. Seismol. Soc. Am.* **110**, 1799–1817, doi: 10.1785/0120200026.

Savran, W. H., J. A. Bayona, P. Iturrieta, K. M. Asim, H. Bao, K. Bayliss, M. Herrmann, D. Schorlemmer, Ph. J. Maechling, and M. J. Werner (2022). pyCSEP: A Python toolkit for earthquake forecast developers. *Seismol. Res. Lett.* **93**, 2858–2870, doi: 10.1785/0220220033.

Schneider, M., A. Wein, S. K. McBride, N. van der Elst, J. S. Becker , R. Castro, M. Diaz, , H. Gonzalez-Huizar, J. Hardebeck, A. J. Michael, L. Mixco, and M. Page (2025). Meet the People Where They Are: Assessing User Needs for Aftershock Forecast Products in El Salvador, Mexico and the United States, *International Journal of Disaster Risk Reduction*, in press, doi: 10.1016/j.ijdrr.2025.105450.

Schwartz, D. P., J. J. Lienkaemper, S. Hecker, K. I. Kelson, T. E. Fumal, J. N. Baldwin, G. G. Seitz, and T. M. Niemi (2014). The earthquake cycle in the San Francisco Bay region: A.D. 1600–2012, *Bull. Seismol. Soc. Am.* **104**, 1299–1328, doi: 10.1785/0120120322.

Segou, M., T. Parsons, and W. Ellsworth (2013), Comparative evaluation of physics-based and statistical forecasts in Northern California, *J. Geophys. Res. Solid Earth* **118**, 6219–6240, doi:10.1002/2013JB010313.

Shaw, B. E., K. R. Milner, E. H. Field, K. Richards-Dinger, J. J. Gilchrist, J. H. Dieterich, and T. H. Jordan (2018). Physics-based earthquake simulator replicates seismic hazard statistics across California, *Science Advances* **4**, eaau0688, doi: 10.1126/sciadv.aau0688.

Shaw, B. E. (2019). Beyond backslip: Improvement of earthquake simulators from new hybrid loading conditions, *Bull. Seismol. Soc. Am.* **109**, 2159–2167, doi: 10.1785/0120180128.

Shaw, B. E. (2023). Magnitude and slip scaling relations for fault based seismic hazard, *Bull. Seismol. Soc. Am.* **113**, 924–947, doi: 10.1785/0120220144.

Shelly, D. R., K. Mayeda, J. Barno, K. M. Whidden, M. P. Moschetti, A. L. Llenos, et al. (2022), A Big Problem for Small Earthquakes: Benchmarking Routine Magnitudes and Conversion Relationships with Coda Envelope-Derived Mw in Southern Kansas and Northern Oklahoma. *Bull. Seismol. Soc. Am.* **112**, 210–225. doi: 10.1785/0120210115.

Spassiani, I, G Falcone, M Murru, W Marzocchi, Operational Earthquake Forecasting in Italy: Validation after 10 yr of operativity, *Geophys. J. Int.* **234**, 2501–2518, doi: 10.1093/gji/ggad256.

Stein, R. S., A. A. Barka, and J. H. Dieterich(1997). Progressive failure on the North Anatolian fault since 1939 by earthquake stress triggering, *Geophys. J. Int.* **128**, 594–604, doi: 10.1111/j.1365-246X.1997.tb05321.x.

Stein, R. S. (2003). Earthquake Conversations, *Scientific American* **288**, 72-79, doi: 10.1038/scientificamerican012003-DipeiQnMaPMOL1RMjOPhi.

Stockman, S., D. J. Lawson, and M. J. Werner (2023). Forecasting the 2016–2017 Central Apennines earthquake sequence with a neural point process, *Earth's Future* **11**, e2023EF003777, doi: 10.1029/2023EF003777.

Thompson Jobe, J., A. E. Hatem, R. Gold, C. DuRoss, N. Reitman, R. Briggs, and C. Collett (2022). Revised earthquake geology inputs for the central and eastern United States and southeast Canada for the 2023 National Seismic Hazard Model. *Seismol. Res. Lett.* **93**, 3100–3120, doi: 10.1785/0220220162.

Tullis, T. E. (2012). Preface to the focused issue on earthquake simulators, *Seismol. Res. Lett.* **83,** 957–958, doi: 10.1785/0220120122.

Uphoff, C., D. A. May, and A.-A. Gabriel (2022). A discontinuous Galerkin method for sequences of earthquakes and aseismic slip on multiple faults using unstructured curvilinear grids, *Geophys. J. Int.* **233**, 586–626, doi: 10.1093/gji/ggac467.

van der Elst, N. J. (2021). B-Positive: A robust estimator of aftershock magnitude distribution in transiently incomplete catalogs, *J. Geophys. Res: Solid Earth* **126**, e2020JB021027, doi: 10.1029/2020JB021027.

van der Elst, N. J. and M. T. Page (2023). a-Positive: A Robust Estimator of the Earthquake Rate in Incomplete or Saturated Catalogs, *J. Geophys. Res. Solid Earth* **128**, e2023JB027089, doi: 10.1029/2023JB027089

Vanneste, K., B. Vleminckx, S. Stein, and T. Camelbeeck (2016). Could M_{max} Be the Same for All Stable Continental Regions?. *Seismol. Res. Lett.* **87**, 1214–1223, doi: 10.1785/0220150203.

Valentini, A., C. B. DuRoss, E. H. Field, R. D. Gold, R. W. Briggs, F. Visini, and B. Pace (2020). Relaxing segmentation on the Wasatch fault zone: Impact on seismic hazard, *Bull. Seismol. Soc. Am.* **110**, 83–109, doi: 10.1785/0120190088.

Wallace, R. E. (1987). Grouping and migration of surface faulting and variations in slip rates on faults in the Great Basin province, *Bull. Seismol. Soc. Am.* **77**, 868–876, doi: 10.1785/BSSA0770030868.

Walton, M. A., L. M. Staisch, T. Dura, J. K. Pearl, B. Sherrod, J. Gomberg, et al. (2021). Toward an integrative geological and geophysical view of Cascadia subduction zone earthquakes. *Annual Review of Earth and Planetary Sciences* **49**, 367-398. https://doi.org/10.1146/annurev-earth-071620-065605

Wange, F. and T. H. Jordan (2014). Comparison of Probabilistic Seismic-Hazard Models Using Averaging-Based Factorization. *Bull. Seismol. Soc. Am.* **104**, 1230–1257, doi: 10.1785/0120130263.

Weldon, R., K. Scharer, T. Fumal, and G. Biasi (2004). Wrightwood and the earthquake cycle: What a long recurrence record tells us about how faults work, *GSA Today* **14**, 4–10, doi: doi: 10.1130/1052- 5173(2004)014<4:WATECW>2.0.CO;2.

Weldon, R. J., II, G. P. Biasi, C. J.Wills, and T. E. Dawson (2007). Overview of the southern San Andreas fault model; Appendix E in the Uniform California Earthquake Rupture Forecast, version 2 (UCERF 2), *U.S. Geol. Surv. Open-File Rept. 2007-1437-E*, and *California Geol. Surv. Special Rept. 203-E*, doi: 10.3133/ofr20071437E.

Woessner, J., S. Hainzl, W. Marzocchi, M. J. Werner, A. M. Lombardi, F. Catalli, B. Enescu, M. Cocco, M. C. Gerstenberger, and S. Wiemer (2011), A retrospective comparative forecast test on the 1992 Landers sequence, *J. Geophys. Res*. **116**, B05305, doi:10.1029/2010JB007846.

Young, Z. M., C. Kreemer, W. C. Hammond, and G. Blewitt (2023). Interseismic Strain Accumulation between the Colorado Plateau and the Eastern California Shear Zone: Implications for the Seismic Hazard near Las Vegas, Nevada, *Bull. Seismol. Soc. Am.* **113**, 856–876, doi: 10.1785/0120220136.

Young, Z. M., C. Kreemer, W. C. Hammond, and G. Blewitt (2023). Interseismic Strain Accumulation between the Colorado Plateau and the Eastern California Shear Zone: Implications for the Seismic Hazard near Las Vegas, Nevada. *Bull. Seismol. Soc. Am.* **113**, 856–876, doi: 10.1785/0120220136

Zaliapin, I., V. Keilis-Borok, and M. Ghil (2003). A Boolean delay model of colliding cascades. I: Multiple seismic regimes, *J. Stat. Phys.* **111**, 815–837, doi: 10.1023/A:1022850215752.

Zaliapin, I., A. Gabrielov, V. Keilis-Borok, and H. Wong (2008). Clustering analysis of seismicity and aftershock identification, *Phys. Rev. Lett.* **101**, 018501, doi: 10.1103/PhysRevLett.101.018501.

Zaliapin, I., and Y. Ben-Zion (2020). Earthquake declustering using the nearest-neighbor approach in space-time-magnitude domain, *J. Geophys. Res.: Solid Earth* **125**, e2018JB017120, doi: 10.1029/2018JB017120.

Zeng, Y., M. D. Petersen, and Z.-K. Shen (2018). Earthquake Potential in California-Nevada Implied by Correlation of Strain Rate and Seismicity, *Geophys. Res. Lett.* **45**, 1778-1785, doi: 10.1002/2017GL075967.

Zeng, Y. (2022a). GPS velocity field of the western United States for the 2023 National Seismic Hazard Model Update, *Seismol. Res. Lett.* **93**, 3121–3134, doi: 10.1785/0220220180.

Zielke, O., D. Schorlemmer, S. Jónnson, and P. M. Mai (2020). Magnitude-dependent transient increase of seismogenic depth, *Seismol. Res. Lett.* **91**, 2182-2191, doi: 10.1785/0220190392.

Zielke, O. and P. M. Mai (2023). MCQsim: A Multicycle Earthquake Simulator, *Bull. Seismol. Soc. Am.* **113**, 889–908, doi: 10.1785/0120220248

Zielke, O. and P. M. Mai (2025). MCQsim: Does Subsurface Fault Geometry Affect Aleatory Variability in Modeled Strike-Slip Fault Behavior?, *Bull. Seismol. Soc. Am.* **115**, 399-415, doi: 10.1785/0120240152

Zöller, G. (2022). A Note on the Estimation of the Maximum Possible Earthquake Magnitude Based on Extreme Value Theory for the Groningen Gas Field, *Bull. Seismol. Soc. Am.* **112**, 1825–1831, doi: 10.1785/0120210307

Zöller, G. (2013). Convergence of the frequency-magnitude distribution of global earthquakes: Maybe in 200 years, *Geophys. Res. Lett.* **40**, 3873–3877, doi: 10.1002/grl.50779.

Zlydenko, O., G. Elidan, A. Hassidim, D. Kukliansky, Y. Matias, B. Meade, A. Molchanov, S. Nevo and Y. Bar-Sinai (2023). A neural encoder for earthquake rate forecasting. *Sci Rep* **13**, 12350, doi: 10.1038/s41598-023-38033-9.

Author Mailing Addresses

Edward H. Field

U.S. Geological Survey, Denver Federal Center

PO Box 25046, MS 966

Denver, CO 80225-0046

Alexandra E. Hatem

U.S. Geological Survey, Denver Federal Center

PO Box 25046, MS 966

Denver, CO 80225-0046

Bruce E. Shaw

Lamont Doherty Earth Observatory

Columbia University

Palisades, NY 10964

Morgan T. Page
U.S. Geological Survey
525 S. Wilson Avenue
Pasadena, CA 91106

P. Martin Mai
King Abdullah University of Science and Technology, KAUST
Thuwal, SAUDI ARABIA

Kevin R. Milner
U.S. Geological Survey
525 S. Wilson Avenue
Pasadena, CA 91106

Andrea L. Llenos
U.S. Geological Survey, Denver Federal Center
PO Box 25046, MS 966
Denver, CO 80225-0046

Andrew J. Michael
Earthquake Science Center
350 N. Akron Rd.
Moffett Field, CA 94035
Office: 650-439-2777

Fred F. Pollitz

Earthquake Science Center
350 N. Akron Rd.
Moffett Field, CA 94035
Office: 650-439-2821

Jessica Thompson Jobe
U.S. Geological Survey, Denver Federal Center
PO Box 25046, MS 966
Denver, CO 80225-0046

Tom Parsons
Pacific Coastal and Marine Science Center
PO Box 158
Moffett Field, CA 94035

Olaf Zielke
King Abdullah University of Science and Technology, KAUST
Thuwal, SAUDI ARABIA

David R. Shelly
U.S. Geological Survey, Denver Federal Center
PO Box 25046, MS 966
Denver, CO 80225-0046

Alice-Agnes Gabriel
IGPP
Scripps Institution of Oceanography
UC San Diego
9500 Gilman Dr #0225
La Jolla, CA 92093-0225

Devin McPhillips
U.S. Geological Survey
525 S. Wilson Avenue
Pasadena, CA 91106

Richard W. Briggs
U.S. Geological Survey, Denver Federal Center
PO Box 25046, MS 966
Denver, CO 80225-0046

Elizabeth S. Cochran
U.S. Geological Survey
525 S. Wilson Avenue
Pasadena, CA 91106

Nicolas Luco
U.S. Geological Survey, Denver Federal Center
PO Box 25046, MS 966
Denver, CO 80225-0046

Mark D. Petersen
U.S. Geological Survey, Denver Federal Center
PO Box 25046, MS 966
Denver, CO 80225-0046

Peter M. Powers
U.S. Geological Survey, Denver Federal Center

PO Box 25046, MS 966
Denver, CO 80225-0046

Justin Rubinstein
Earthquake Science Center
350 N. Akron Rd.
Moffett Field, CA 94035
Office: 650-439-2821

Allison M. Shumway
U.S. Geological Survey, Denver Federal Center
PO Box 25046, MS 966
Denver, CO 80225-0046

Nicholas J. van der Elst
U.S. Geological Survey
525 S. Wilson Avenue
Pasadena, CA 91106

Yuehua Zeng
U.S. Geological Survey, Denver Federal Center
PO Box 25046, MS 966
Denver, CO 80225-0046

Christopher B. Duross
U.S. Geological Survey, Denver Federal Center
PO Box 25046, MS 966
Denver, CO 80225-0046

Jason M. Altekruse
U.S. Geological Survey, Denver Federal Center
PO Box 25046, MS 966
Denver, CO 80225-0046

Tables

None.

List of Figures Captions

Figure 1. Regions where the U. S. Geological Survey issues National Seismic Hazard Models (NSHMs).

Figure 2. A depiction of the U. S. Geological Survey (USGS) earthquake hazard and risk forecasting enterprise, including the disciplinary science categories (top), the system-level predictive models (middle), and some USGS forecasting products (bottom). UCERF3-ETAS is the fully time-dependent earthquake rupture forecast published by Field et al. (2021) and FEMA P366 is the nationwide earthquake risk analysis of Jaiswal et al. (2023).

Figure 3. Illustration of time-dependent vs fully time-independent models. The lower panel shows the monthly rate of $M \geq 2.5$ events in California over a 100-year simulation window, with red and black depicting the time-dependent and time-independent rates, respectively. The top panel shows

the timing of $M \geq 6$ events for each model (with circle size varying with magnitude). The time-dependent simulation is based on the UCERF3-ETAS model (Field et al., 2021), for which aftershock sequences can be seen following larger events. The time-independent model is based on the same set of events, but with event times randomized to mimic a Poisson process. Changes in $M \geq 2.5$ rates for the time-dependent (red) model are a good proxy for the change in large-event probabilities. Note that rates (and probabilities) can increase by more than an order of magnitude following large events and can also be lower by a factor two during quiet times, relative to the Poisson approximation.

Figure 4. Earthquake Rupture Forecast (ERF) main modeling components.

Figure 5. An illustration of the inversion-based fault system solution. The fault system is subdivided into a number of subsections and viable fault ruptures are defined as occurring on a set of these subsections. The rate or frequency of each rupture (f_r) is then determined by solving a set of equations based on various data constraints.

Figures

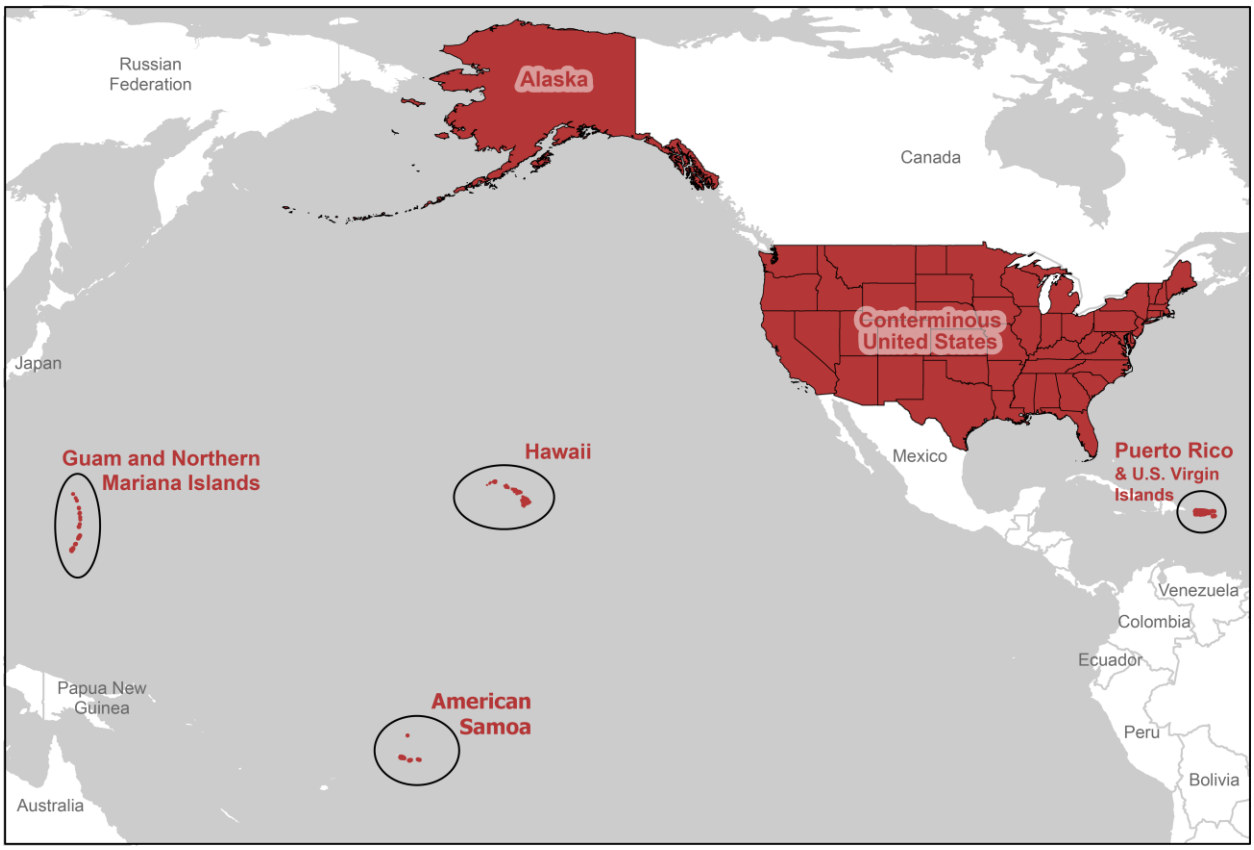

Figure 1. Regions where the U. S. Geological Survey issues National Seismic Hazard Models (NSHMs).

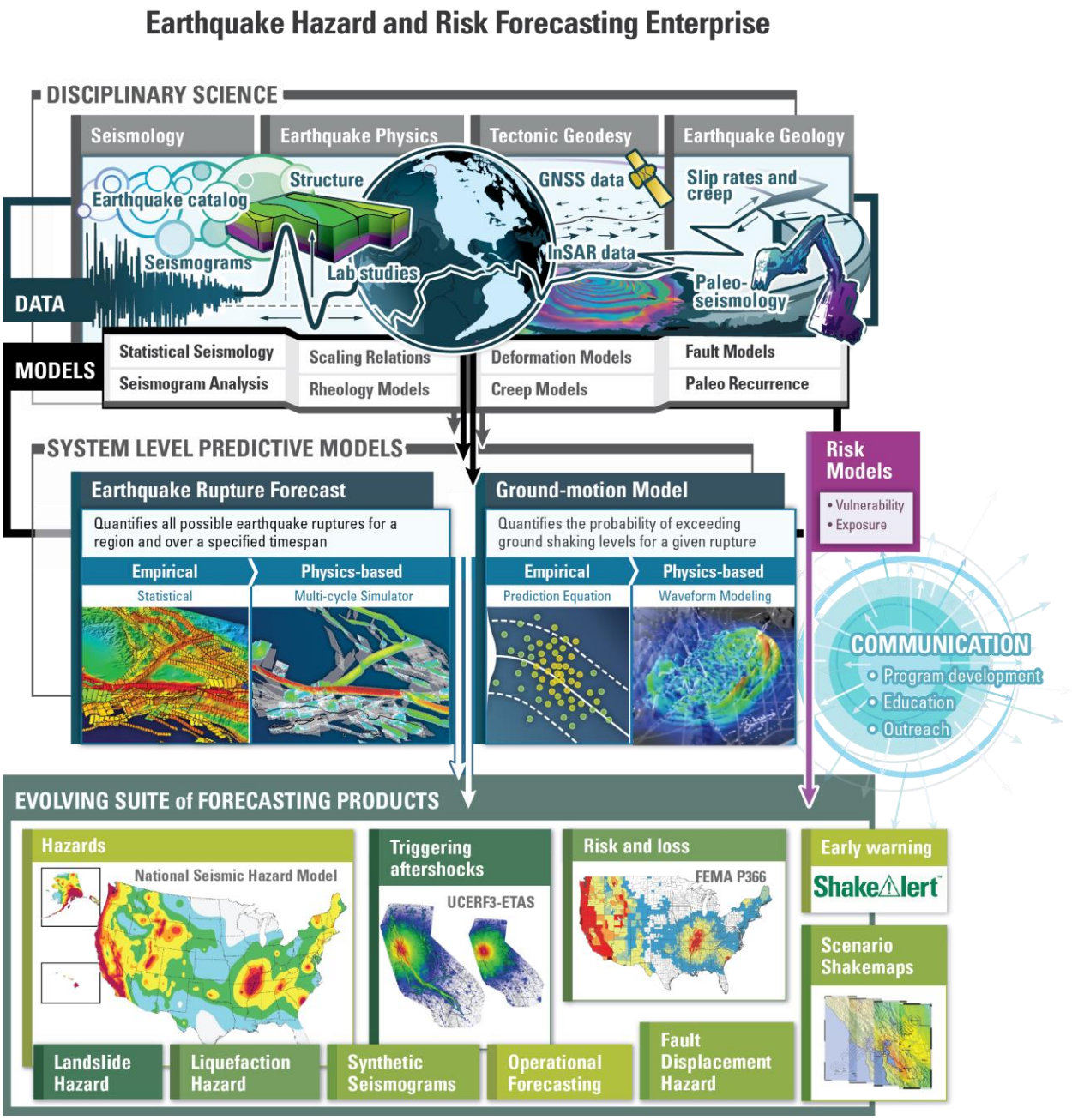

Figure 2. A depiction of the U. S. Geological Survey (USGS) earthquake hazard and risk forecasting enterprise, including the disciplinary science categories (top), the system-level predictive models (middle), and some USGS forecasting products (bottom). UCERF3-ETAS is the fully time-dependent earthquake rupture forecast published by Field et al. (2021) and FEMA P366 is the nationwide earthquake risk analysis of Jaiswal et al. (2023).

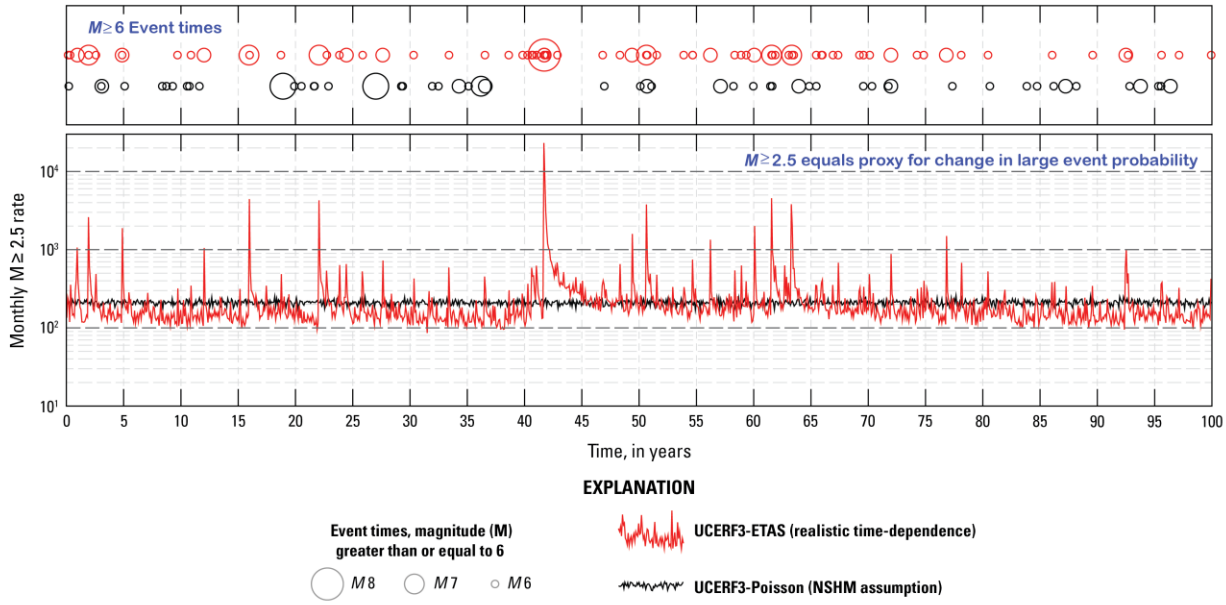

2333

2334 **Figure 3.** Illustration of time-dependent vs fully time-independent models. The lower panel shows
2335 the monthly rate of *M*≥2.5 events in California over a 100-year simulation window, with red and
2336 black depicting the time-dependent and time-independent rates, respectively. The top panel shows
2337 the timing of *M*≥6 events for each model (with circle size varying with magnitude). The time-
2338 dependent simulation is based on the UCERF3-ETAS model (Field et al., 2021), for which aftershock
2339 sequences can be seen following larger events. The time-independent model is based on the same
2340 set of events, but with event times randomized to mimic a Poisson process. Changes in *M*≥2.5 rates
2341 for the time-dependent (red) model are a good proxy for the change in large-event probabilities.
2342 Note that rates (and probabilities) can increase by more than an order of magnitude following large
2343 events and can also be lower by a factor two during quiet times, relative to the Poisson
2344 approximation.

2345

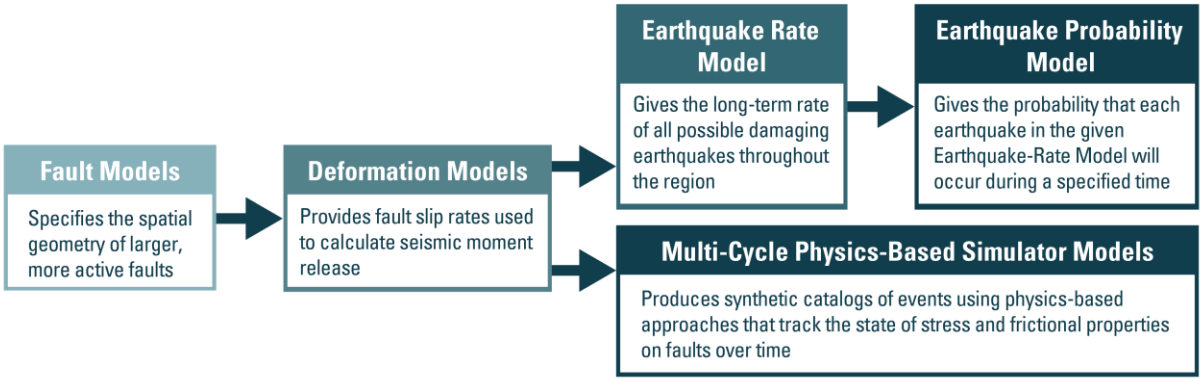

Figure 4. Earthquake Rupture Forecast (ERF) main modeling components.

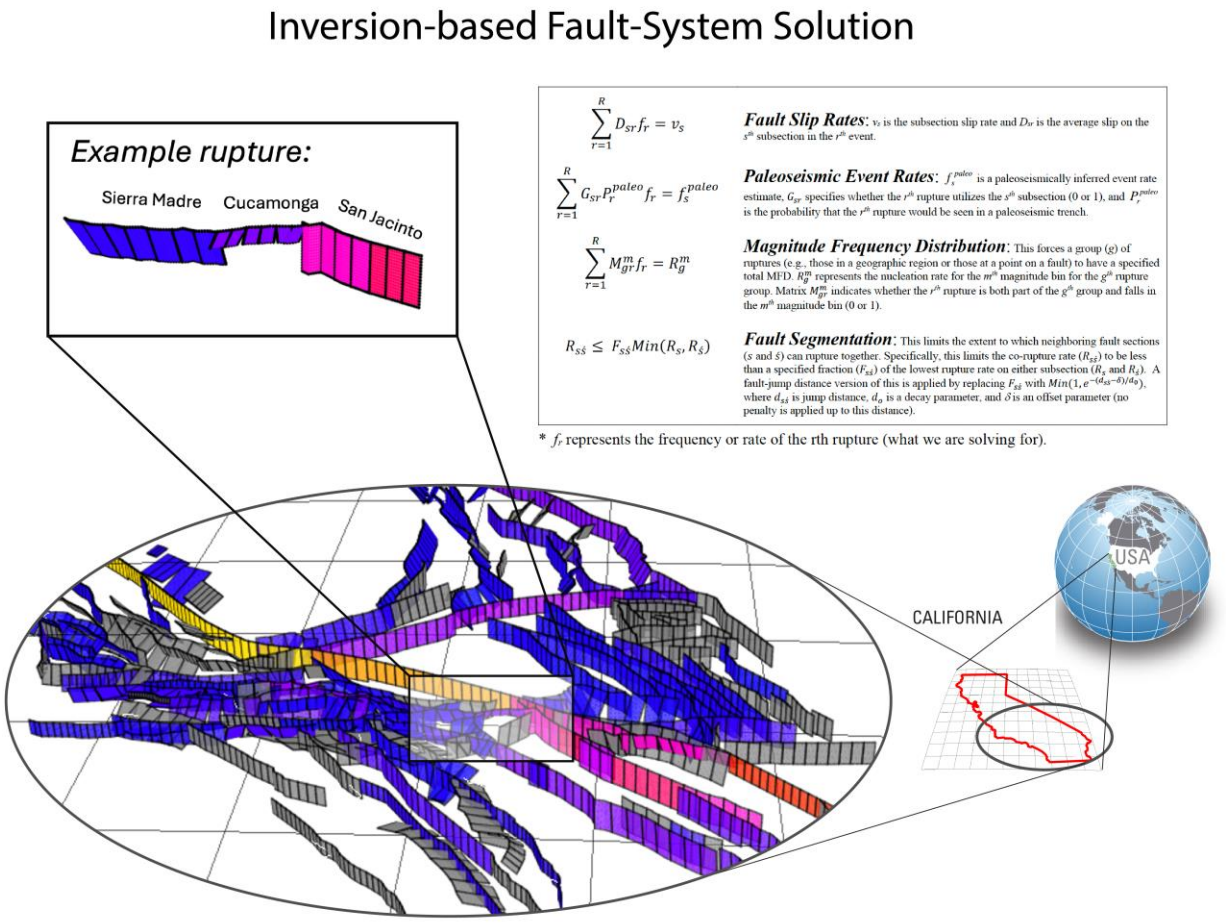

Figure 5. An illustration of the inversion-based fault system solution. The fault system is subdivided into a number of subsections and viable fault ruptures are defined as occurring on a set of these subsections. The rate or frequency of each rupture (f_r) is then determined by solving a set of equations based on various data constraints. The fault model depicted is for California and comes from Field et al. (2014).

Figure 1

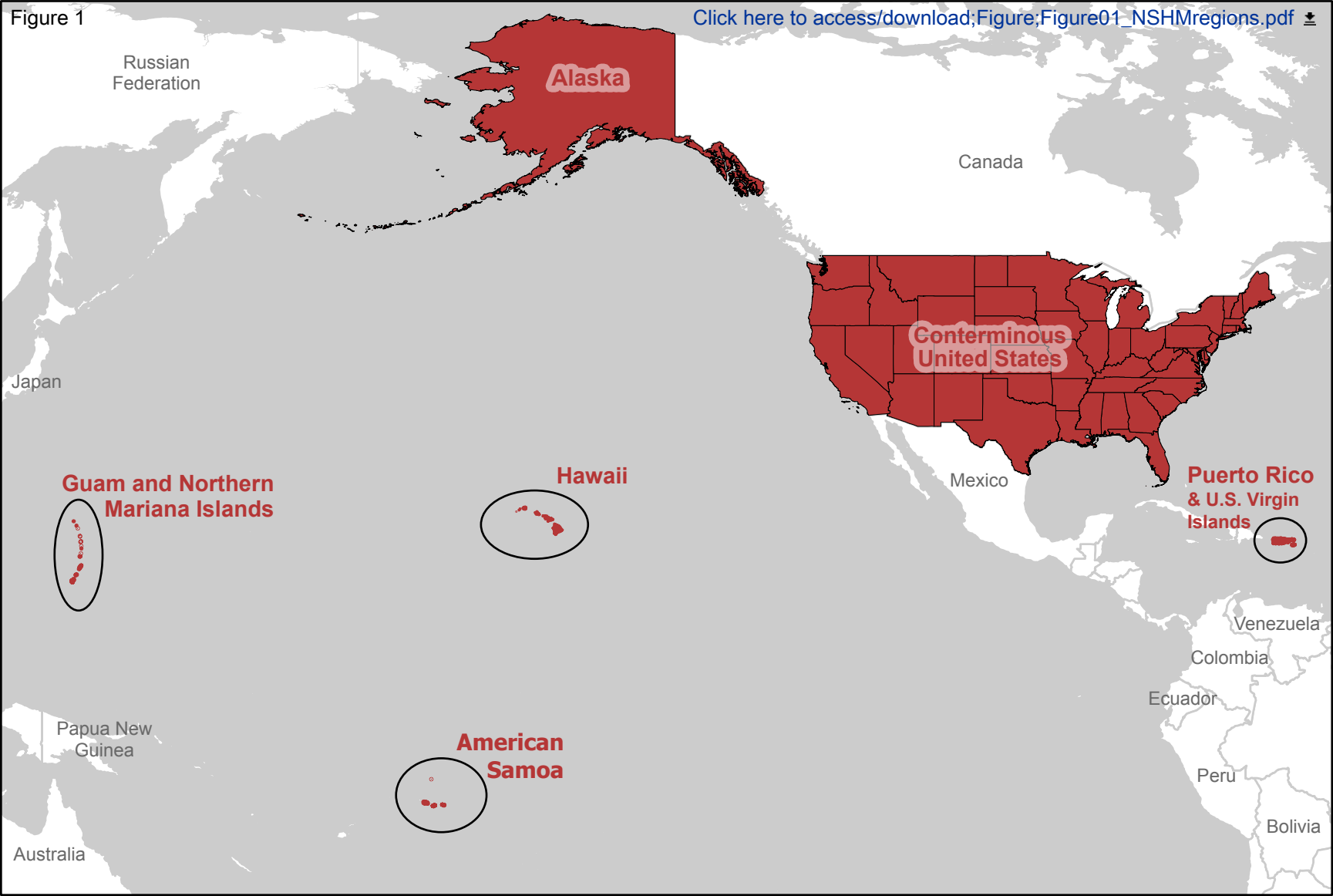

Figure 3

Click here to access/download;Figure;Figure03_TimeDependence.pdf

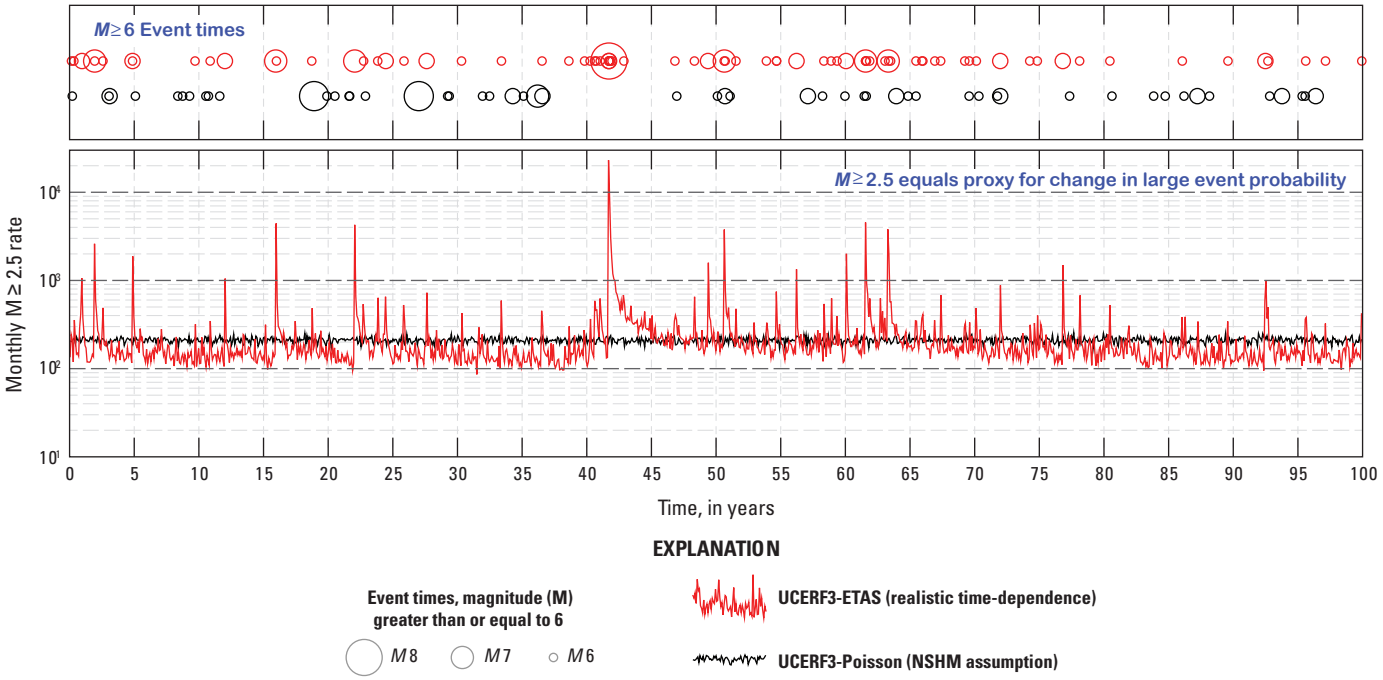

EXPLANATION

Event times, magnitude (M) greater than or equal to 6

M 8 *M* 7 *M* 6

UCERF3-ETAS (realistic time-dependence)

UCERF3-Poisson (NSHM assumption)

Figure 4

Click here to access/download;Figure;Figure04_MainModelComponents.pdf

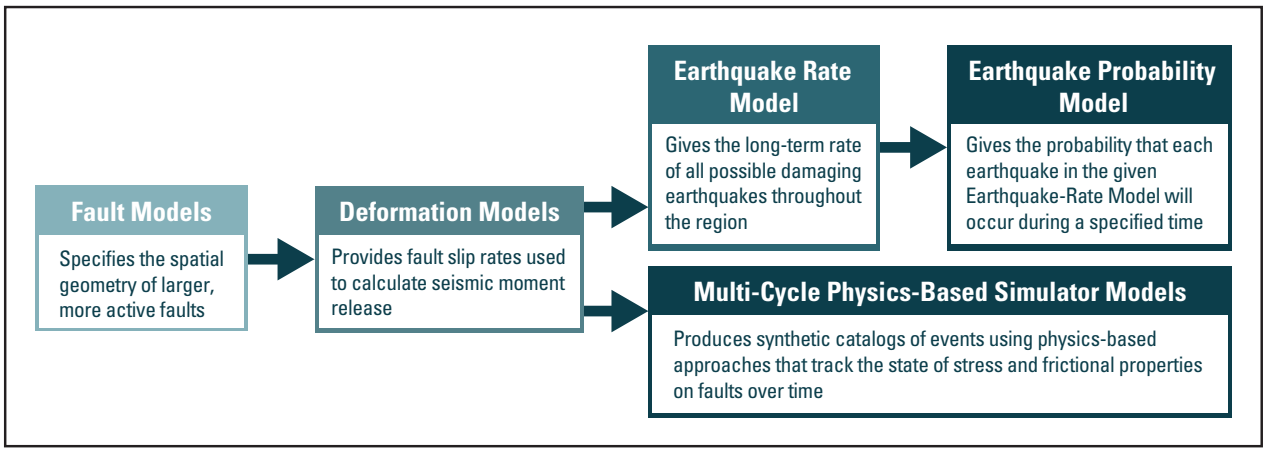

Figure 5

Click here to access/download;Figure;Figure05_FSS-Inversion.pdf

Inversion-based Fault-System Solution

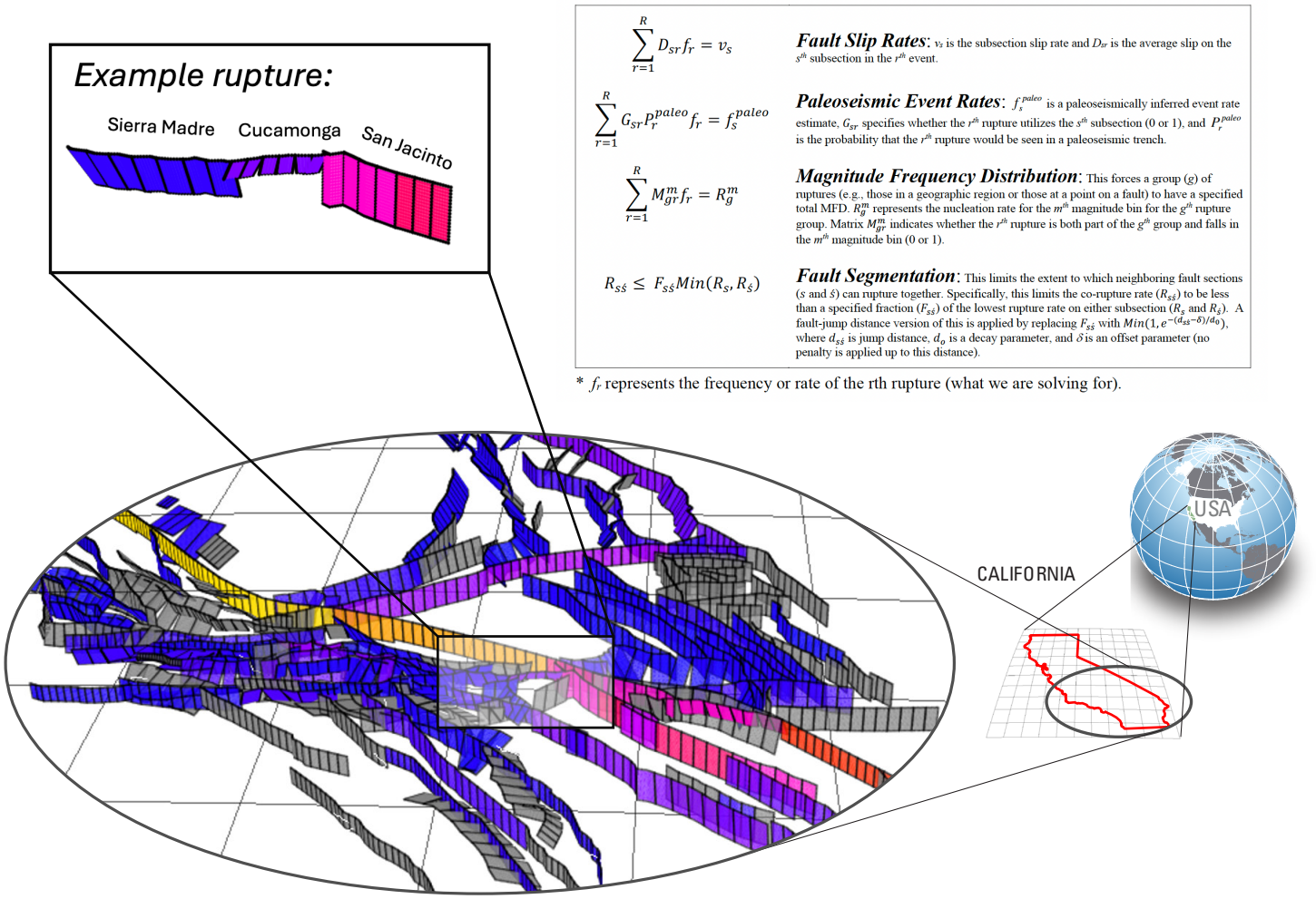

$$\sum_{r=1}^{R} D_{sr} f_r = v_s$$

Fault Slip Rates: v_s is the subsection slip rate and D_{sr} is the average slip on the s^{th} subsection in the r^{th} event.

$$\sum_{r=1}^{R} G_{sr} P_r^{paleo} f_r = f_s^{paleo}$$

Paleoseismic Event Rates: f_s^{paleo} is a paleoseismically inferred event rate estimate, G_{sr} specifies whether the r^{th} rupture utilizes the s^{th} subsection (0 or 1), and P_r^{paleo} is the probability that the r^{th} rupture would be seen in a paleoseismic trench.

$$\sum_{r=1}^{R} M_{gr}^{m} f_r = R_g^m$$

Magnitude Frequency Distribution: This forces a group (g) of ruptures (e.g., those in a geographic region or those at a point on a fault) to have a specified total MFD. R_g^m represents the nucleation rate for the m^{th} magnitude bin for the g^{th} rupture group. Matrix M_{gr}^m indicates whether the r^{th} rupture is both part of the g^{th} group and falls in the m^{th} magnitude bin (0 or 1).

$$R_{s\acute{s}} \leq F_{s\acute{s}} Min(R_s, R_{\acute{s}})$$

Fault Segmentation: This limits the extent to which neighboring fault sections (s and $\acute{s}$) can rupture together. Specifically, this limits the co-rupture rate ($R_{s\acute{s}}$) to be less than a specified fraction ($F_{s\acute{s}}$) of the lowest rupture rate on either subsection (R_s and $R_{\acute{s}}$). A fault-jump distance version of this is applied by replacing $F_{s\acute{s}}$ with $Min(1, e^{-(d_{s\acute{s}}-\delta)/d_0})$, where $d_{s\acute{s}}$ is jump distance, d_o is a decay parameter, and δ is an offset parameter (no penalty is applied up to this distance).

* f_r represents the frequency or rate of the rth rupture (what we are solving for).

Figure 2